29 May 1967

To: EEC and NPRC

ADDENDUM TO THE $\Delta Q = \Delta S$ RULE IN LEPTONIC DECAYS PROPOSAL

(Dated 15 th Nov. 1966)

V.Bisi, G.C.Bonazzola, E.Chiavassa
S.Costa, M.I.Ferrero, C.Grosso

(I.N.F.N. - University of Turin)

TABLE OF CONTENTS

SUMMARY.

An experiment is proposed to test the validity of the $\Delta Q = \Delta S$ rule by studying the time distribution of K° leptonic decays.

If the presence of both f ($\Delta Q = \Delta S$) and g($\Delta Q = -\Delta S$) amplitudes is proved, the same distribution is also sensitive to a CP violation in this type of decay.

The proposed experimental apparatus is discussed. The obtainable rates of events and the level of background signals are evaluated. It is found that

a) it is possible to collect a statistics of the order of 1000 event/day

b) call $x = g/f$. Then using a sample of 10^4 events the Re x can be determined with an accuracy of $\pm$ 2% and Im x with an accuracy of $\pm$ 4%.

The evaluation of the event rate is based on some assumptions about the charge exchange K^+ - nucleus cross section. A preliminary test measurement , with different target nuclei,would give very useful information on the charge exchange differential cross section and would allow us to check the validity of the above assumptions.

For this purpose the spectrometer (magnet + spark chambers) that is presently used for the $K_1^\circ - K_2^\circ$ interference experiment by the CERN group, could be placed on the M4 beam, parasyting the present experiments.

The cross section will be determined analyzing $K_1^\circ \to 2\pi$ events. Scan and measurement could be done by Luciole, using the reconstruction and analysis programs already existing.

1. Introduction

The decay modes

$$K^0 \to \pi^- \ell^+ \nu \qquad (f)$$
$$K^0 \to \pi^+ \ell^- \bar{\nu} \qquad (f^*)$$

are allowed by the $\Delta Q = \Delta S$ rule, whereas

$$K^0 \to \pi^+ \ell^- \nu \qquad (g^*)$$
$$K^0 \to \pi^- \ell^+ \bar{\nu} \qquad (g)$$

are forbidden by the same rule but allowed by a $\Delta Q = -\Delta S$ rule. Let f, f*; g, g* be the form factors related to the corresponding amplitudes (as indicated above).

Given an initially pure K^0 beam, the decay rates for $\pi^- e^+ \bar{\nu}$ and $\pi^+ e^- \nu$ modes, expressed as a function of time, are respectively[6]

$$R^+ = \text{Const}\left[|1+x|^2 e^{-t/\tau_2} + |1-x|^2 e^{-t/\tau_1} + 2\left(1-|x|^2\right)\cos\Delta m t\, e^{-(t/2)(1/\tau_1+1/\tau_2)} - 4\,\mathrm{Im}\,x \sin\Delta m t\, e^{-(t/2)(1/\tau_1+1/\tau_2)}\right] \quad (1.1$$

$$R^- = \text{Const}\left[|1+x|^2 e^{-t/\tau_2} + |1-x|^2 e^{-t/\tau_1} - 2\left(1-|x|^2\right)\cos\Delta m t\, e^{-(t/2)(1/\tau_1+1/\tau_2)} - 4\,\mathrm{Im}\,x \sin\Delta m t\, e^{-(t/2)(1/\tau_1+1/\tau_2)}\right] \quad (1.2$$

where $x = \frac{a}{f} = |x|\ e^{i\phi}$

$$m = m_{K_1^0} - m_{K_2^0} = 0.445\,\tau_1^{-1} \quad (7)$$

τ_1 and τ_2 are the lifetimes of the short and long lived K^0.

A value of $x \neq 0$ implies a violation of $\Delta Q = \Delta S$

CP - conservation (in leptonic decays) implies $\phi = 0$.

It follows that if $\Delta Q = \Delta S$ rule is found to be violated ($x \neq 0$) then a test of CP-invariance in leptonic decays is possible.

Present experimental knowledge on this question is summarizd in Table 1 and Fig. 1.

All experiments carried out so far are affected by large errors, both statistical and systematic ones. In particular it is worth noting that:

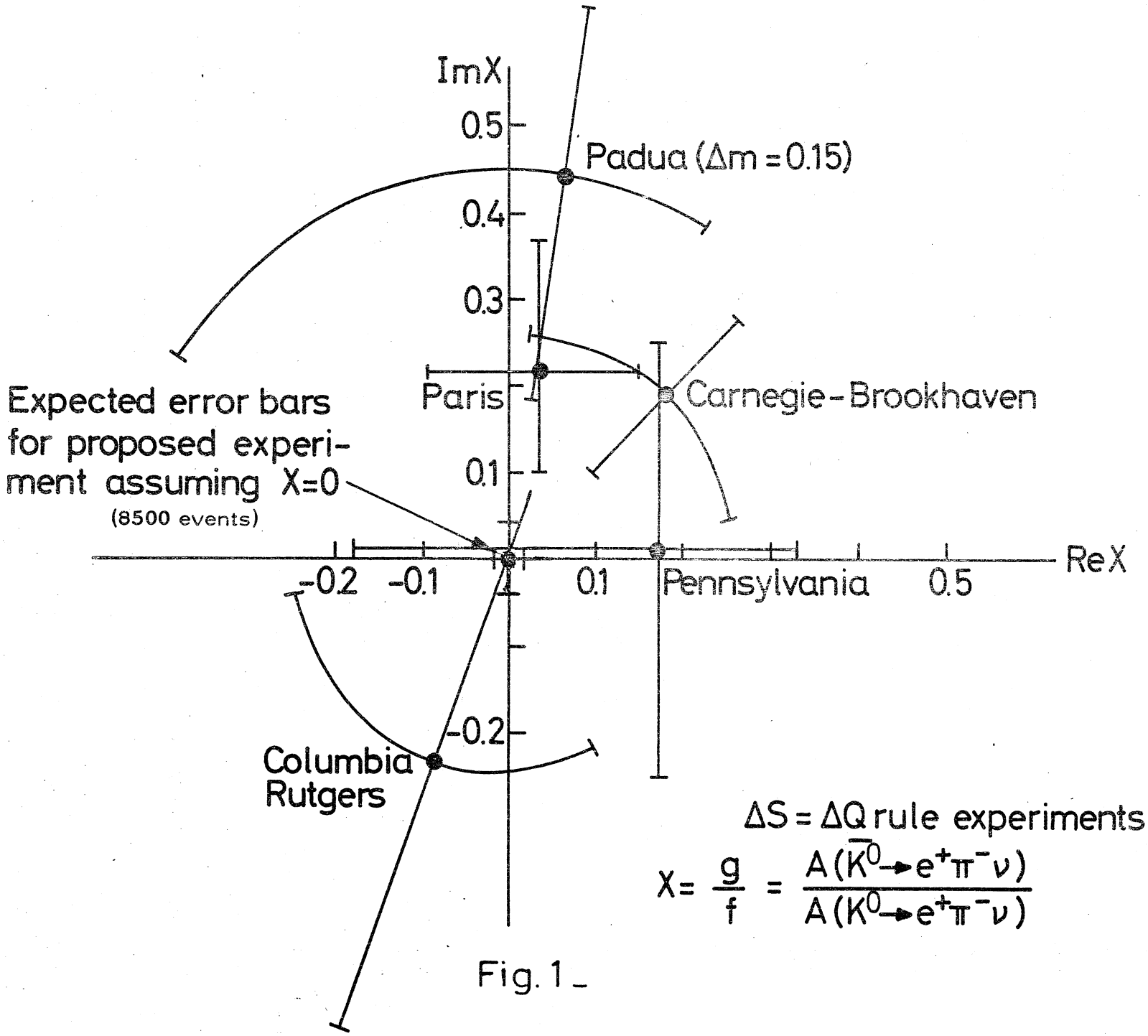

$\Delta S = \Delta Q$ rule experiments

$$X = \frac{g}{f} = \frac{A(\bar{K}^0 \to e^+ \pi^- \nu)}{A(K^0 \to e^+ \pi^- \nu)}$$

Fig. 1

TABLE 1 (from Cabibbo's report at the Berkeley Conference 1966)

Ref.	Technique	Re x	Imx
Paris (1)	Fr BC		
PL 17,59 (65)	$K^+n \to K^\circ p$	$.04^{+.11}_{-.13}$	$.21^{+.15}_{-.11}$
Padua (2)	Fr BC		
N.C 38,684(65)	$K^+n \to K^\circ p$	$.06 \pm .25$	$\pm .43 \pm .25$
Columbia (3)	HBC		
PR. 140,127(65)	$pp \to K^\circ \bar{K}^\circ$	$.07 \pm .2$	$.23 \pm .2$
Carnegie-Brookhaven Tech (4)	D_2 BC		
	$K^+n \to K^\circ p$	$.18^{+.10}_{-.14}$	$.19^{+.14}_{-.12}$
Pennsylvania (5)	SprK		
	$\bar{p}p \to K^\circ \Lambda^\circ$	$.187^{+.16}_{-.35}$	$.0 \pm .25$

a) in experiments performed with a propane-freon bubble chamber (1,2) the momentum of the K°'s could not be determined directly. Only the average value could be established, on a distribution which was spread over an interval of $\sim \pm$ 30% of its average.

Thus the "life time" of each individual K° observed to decay was uncertain by the same amount.

Moreover, in a non negligible number of cases, an unambiguous association of the decay products with the parent interaction producing the K° was not possible.

b) On the other hand, experiments performed with hydrogen or deuterium bubble chambers (3, 4), fast pions, muons and electrons are in general undistinguishable.

Leptonic decays are selected on the basis of kinematical analysis upon all 2 body decays of neutral K°'s. Even so,

the identity of the lepton (and so its charge) cannot be established in general.

Finally, in either cases the collection of large statistics implies long and difficult work in the analysis of the photograms.

To overcome these difficulties, an experiments is proposed based on wire chambers and counters. As compared to bubble chamber work, the use of these techniques would allow more precise determination of the kinematics of the K° decays and yield results of much larger statistical weight in a considerably shorter time.

2. Description of the experiment.

The experimental apparatus, which is proposed to measure the temporal distribution of the K° leptonic decays, is designed to obtain

a) a good momentum resolution ($< 5\%$) of the primary K° beam

b) unambiguous identification of the decay mode

c) a large angular acceptance of the recording system to ensure the collection of large statistics.

K°'s will be produced by "charge exchange" scattering of K^+ on neutrons of complex nuclei. As an example, we have considered a target, formed by five, 1-cm thick, copper plates, separated by 1-cm thick scintillators (Fig. 5, inset 2).

The K°'s thus produced will be allowed to decay in a space corresponding to $6\ \tau_1$ (τ_1 = lifetime of K_1°). For longer times the initially pure K° beam has decayed into an almost pure K_2° beam and the rates R^+, R^- become practically insensitive to the value of x. (see 1.1, 1.2 and Fig. 2). For K° momenta of ~ 2.5 GeV/c, $6\ \tau_1$ corresponds to ~ 80 cm.

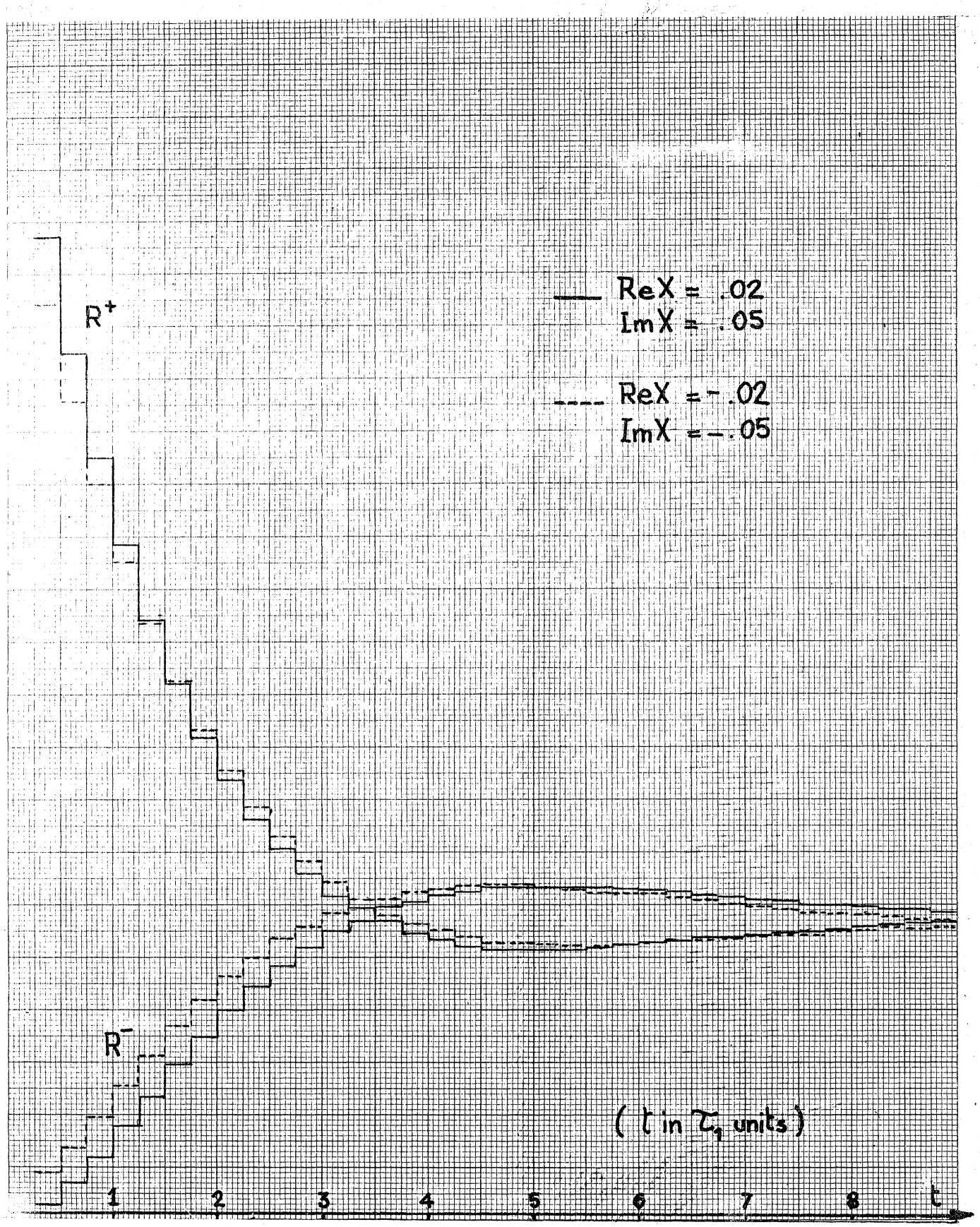

Fig. 2. Time dependence of R^+ R^- for two different values of the parameter x

Charged decay products which have the appropriate geometry, will traverse a spectrometer formed by a system of wire chambers and a wide gap magnet, in which their momentum is determined.

The final counter system (region D in Fig. 3), placed after the spectrometer, divides the solid angle viewed by the decay products, into 4 quadrants. Each quadrant is covered by a scintillator followed by a gas Cerenkov, adjusted to record electrons only.

To select $K^{\circ} \rightarrow \pi + e + \nu$ events it is required that two particles enter two separate quadrants but one and only one triggers the gas Cerenkov counter.

The spectrometer and the electron detector (Region C and D in Fig. 3) have been built by the CERN-Aachen groups and are been tested in the PS .

The Turin group will build :

1) the detectors designed to separate K^{+} from the rest of the beam. This consists of two gas threshold Cerenkov counters and three scintillators.

2) The copper target with the counter system designed to determine the position of the K° production.

3) All the electronics related to the above system of counters.

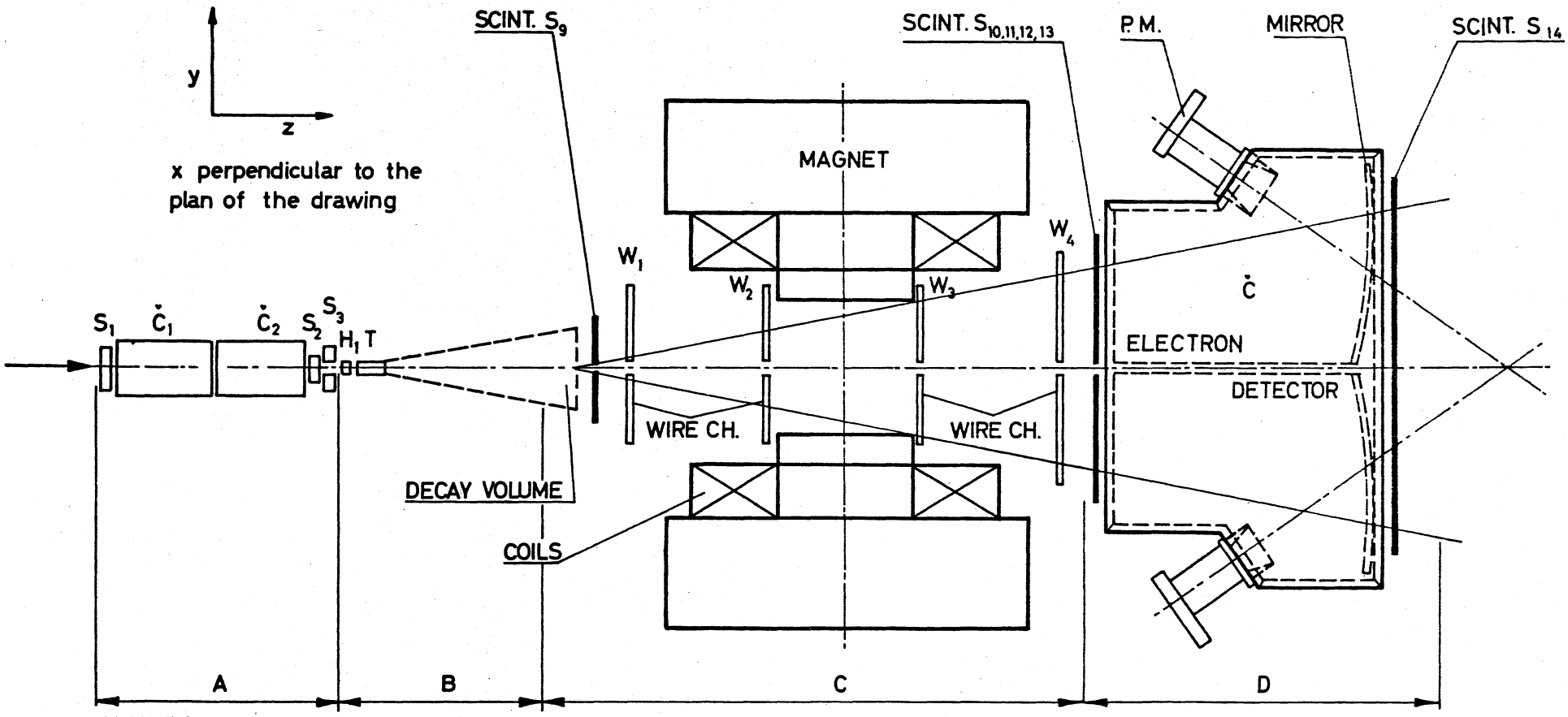

Fig. 3. The experimental apparatus. The part beam definition-target (regions A, B), described in detail in this report, will be set up at Turin. The instrumentation forming the spectrometer and the electron detector constructed, by the Rubbia group, is under test at Cern.

3. The beam and the experimental apparatus

The experimental apparatus was designed to provide the discrimination of Kaons against pions and protons background (to take into account the possibility of an unseparated K^+ beam, if a separated one will not be available).
The assumed beam features are:

K^+ mean momentum	2.5 GeV/c
momentum spread $\frac{\Delta p}{p}$	$= \pm$ 2%
angular spread	$\pm$ .006 rad
intensity	10^5 K^+/pulse

The beam will be focused on a rectangular spot $\sim$ 0.5 x 1.5 cm^2 in front of the target.

The apparatus is described in Fig. 3.

Part A - is required to determine the trajectories of the incoming K^+ and separate kaons from pions and protons.

The discrimination from the background of other particles will be obtained by the two hethylene filled Čerenkov counters ($\check{C}_1$ and $\check{C}_2$ in Fig. 3 and 5). $\check{C}_1$ is 40 cm long and 15 cm in diameter; $\check{C}_2$ equally long and 12 cm in diameter. The first with be filled to 10 atms which corresponds to a threshold velocity β = 0,993. Using a beam 2.5 GeV/c in momentum, this counter will record only pions. $\check{C}_2$ will be filled to 35 atms and will record both Kaons and pions of the same momentum.

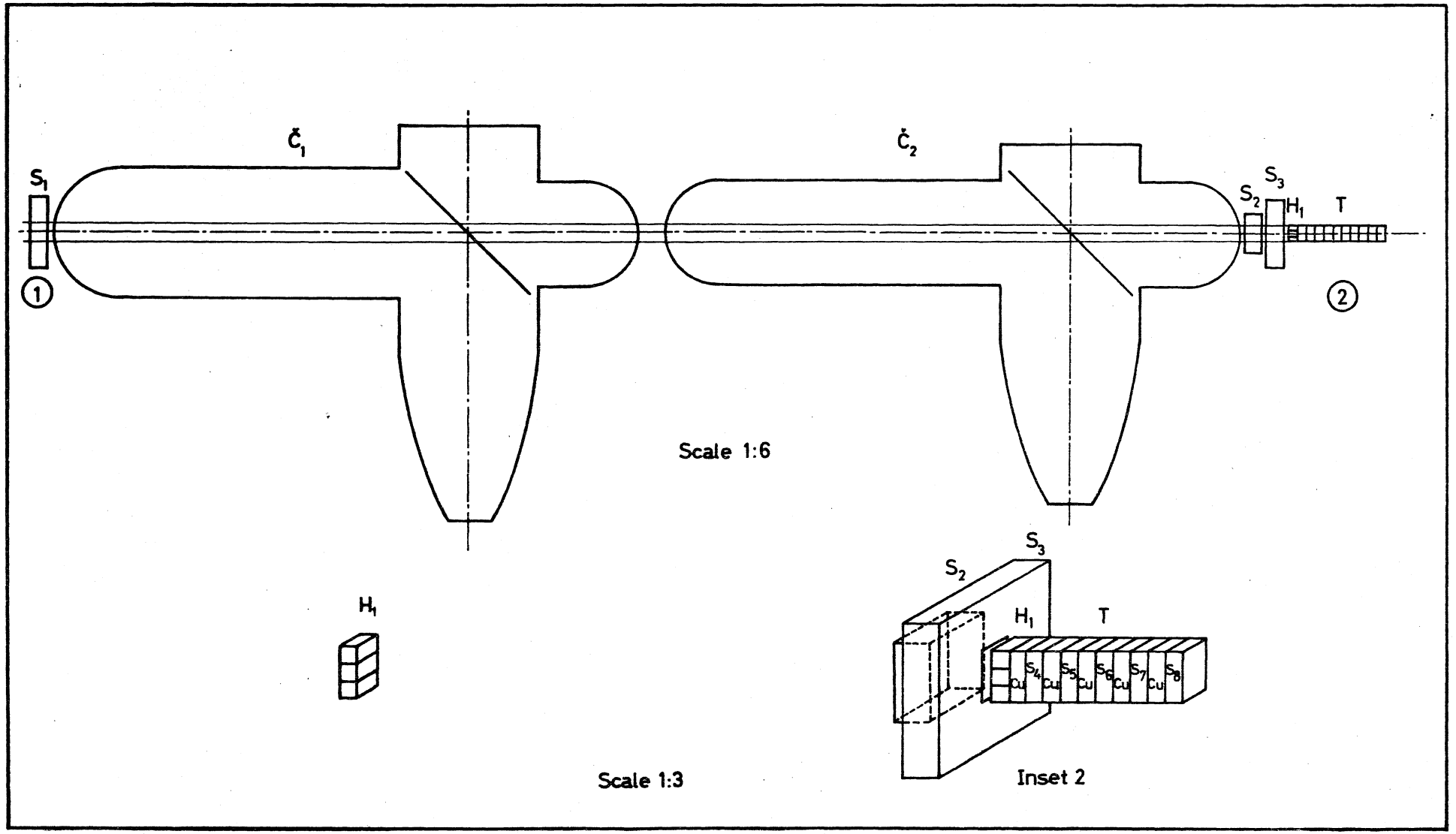

Fig. 5 . Details of the experimental apparatus.

Thus the individuation of the Kaons is clearly possible.

Counters S_1 S_2 are scintillation counters used as beam monitors; S_3 is introduced to limit the size of the beam. It has a rectangular hole of 0.5 x 1.5 cm^2 and it anti-coincides stray particles at large angles.

Part B - contains the hodoscope H_1 and the target (see inset 2 in Fig. 5) and the system of counters which are required to determine the origin of the K°. The hodoscope is made of 3 scintillators, arranged as indicated in Fig. 5. Each scintillator presents to the beam a total surface of $\Delta x \cdot \Delta y = 0.5 \times 0.5$ cm^2. Thus the intersection of a trajectory with the plane of the hodoscope is determined with a precision of $\Delta x = \pm 0.25$ $\Delta y = \pm 0.25$.

The target is formed by five 1 cm thick plates of copper, separated by 1cm thick plastic scintillators. Copper was selected as a medium giving comparatively high production of K°'s and relatively low coulomb scattering on the primary K^+. Signals from each scintillator are analyzed in amplitude, digitized by a fast pulse encoder and stored in a buffer memory.

Thus the Z-coordinate (see Fig. 3) of the charge-exchange interaction is determined to $\pm$ 0.5 cm. The x and y coordinates are determined extrapolating the K^+ direction, which will be known to within $\pm$ 6 mr at the entry into the target. Due to multiple scattering in the copper target, the precision in x and y decreases when z increases. For instance for a K^+ which interact on the last plate, the uncertainly in its direction is $\sim$0.02 rad, corresponding to a maximum deplacement of 0.2 cm.

The spectrometer (Part C(*)) is formed by a wide gap magnet. The gap presents a cross section 2 m. wide and 0.3 ⟝

(*) part C and part D, have been built by the CERN-Aachen group.

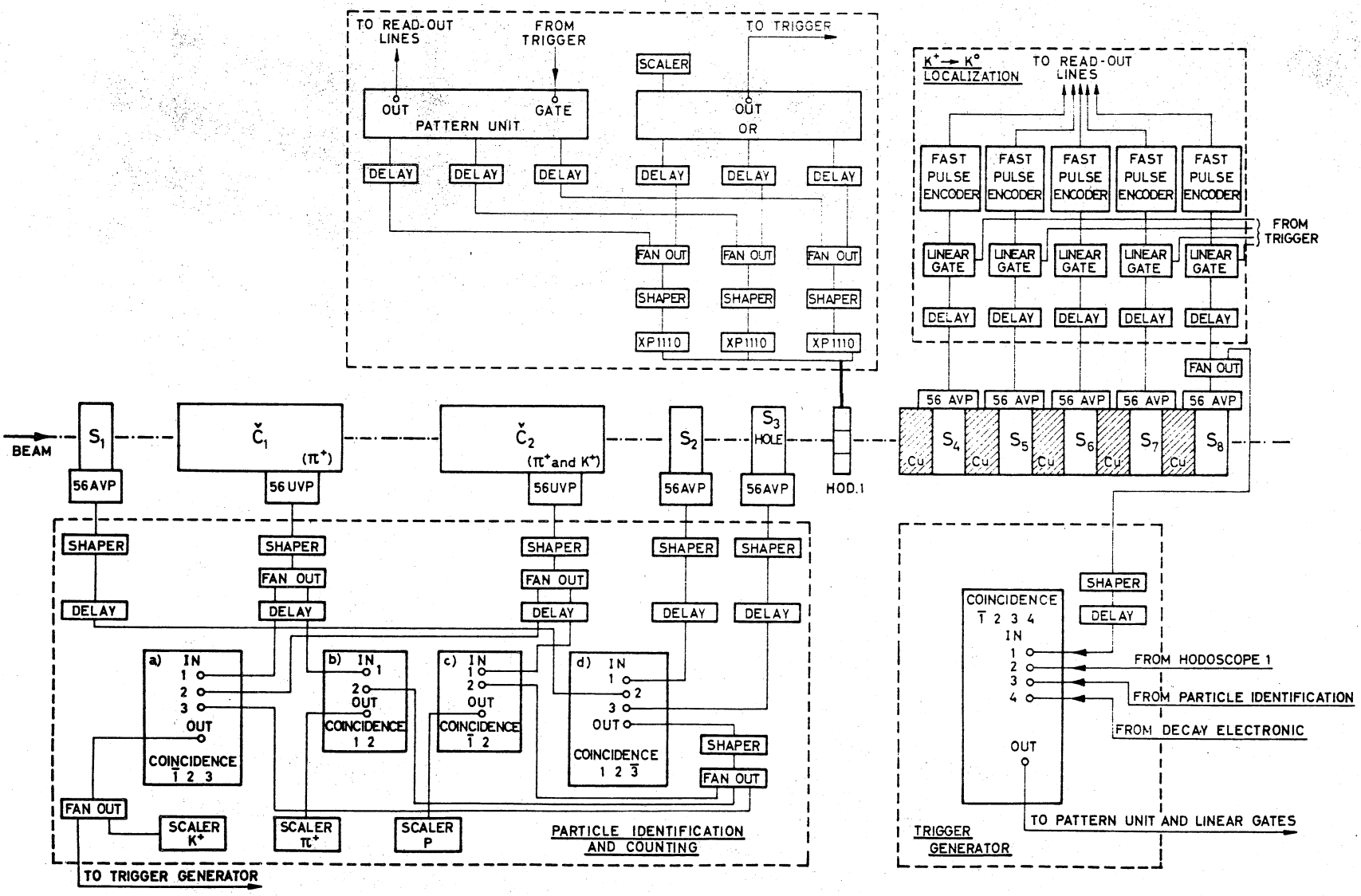

Fig. 6. Block diagram of the electronic apparatus (parts A, B).

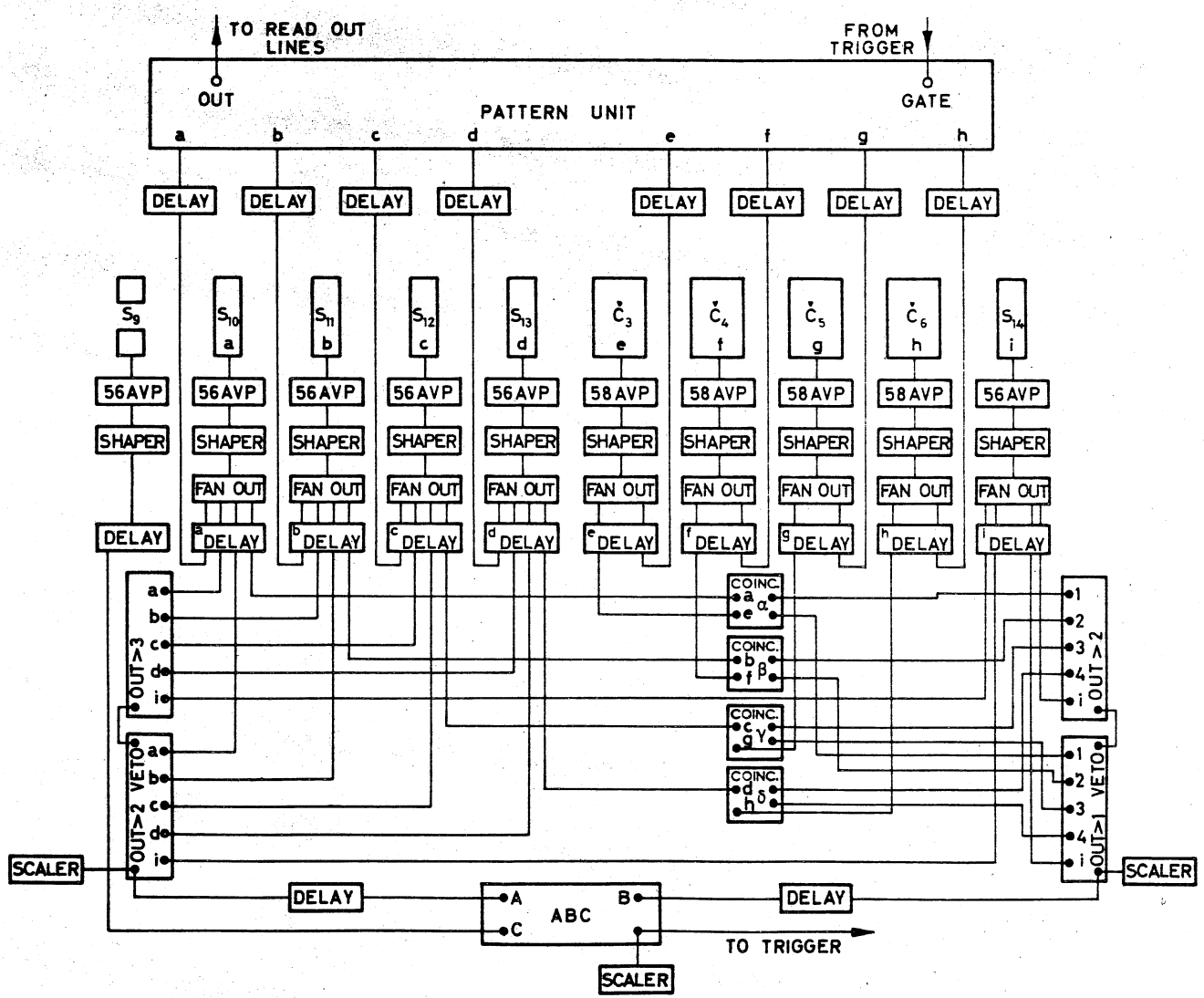

Fig. 7. Block diagram of the electronics apparatus (parts C, D).

the shaped pulses from the x associated Čerenkov counters; the outputs of the coincidences are fed into a circuit performing the logic function of an EXCLUSIVE OR. Let's call B its possible output. On the other hand, signals from $S_{10} \div S_{13}$ are also sent to two majority coincidences. One of these (≥ 2) is inhibited by the output of the other one (> 3). The output of the first VOTER, say A, is fed into a three-fold coincidence together with pulses B and C. The latter comes from the "drilled" scintillator S_9. The event ABC indicates a useful decay, and the corresponding pulse is therefore sent to the trigger generator (see Fig. 6). Finally, when a trigger occurred, the pulses from $S_{10} \div S_{13}$ and from $\check{C}_3 \div \check{C}_6$ are also stored in a pattern unit, thus enabling the subsequent labelling of the trajectories seen by the wire chambers.

4. Montecarlo estimates of the efficiency of the apparatus

In this section we shall briefly describe a Montecarlo calculation performed in order to

a) optimize the geometrical efficiency of the apparatus

b) evaluate the experimental errors

c) subtract the background

d) calculate the event rates.

a) Production and efficiency

A K^+ beam of 2.5GeV/c($\pm$ 2%),with an angular spread $\delta_{K^+} = \pm$ 6 mrad,inpinges on the copper target. For each K^+ the z coordinate of the interaction is chosen at random froma uniform distribution over the 5 plates of the target. The other two coordinates, x and y, are derived from the distribution of the trajectories of the K^+ in the beam, taking into account the spread of the incident beam as well as the Coulomb scattering in the copper plates. The K°'s are produced both in "elastic"

$$K^\circ + (n) \rightarrow K^\circ + p \qquad 4.1$$

as well as in inelastic reactions ((n) indicates a bound neutron)

We consider elastic production at first, and we shall evaluate later the inelastic one, which gives rise to a unwanted background.

The angular distribution of the K°'s is determined by

- the angular and momentum distribution of the K^+
- the Fermi motion of the target nucleons. We have assumed a distribution function

$$dN \propto p^2 \exp(-p^2/p_o^2)\, dp \qquad (p_o = 165 \text{ MeV/c})$$

- the cross section $d\sigma/d\Omega_{K^\circ}$ for reaction 4.1. We have taken experimental results for charge exchange scattering of K^+ of comparable energy on deuterium (Fig.8) and assumed that in the C.M. system $d\sigma/d\Omega_{K^\circ}$ did not depend critically on the energy.

The angular and momentum distributions of the K° thus produced and recorded by the apparatus are given in Fig. 9+10. The distribution of the recoil proton ranges, projected along the beam direction, is shown in fig.11. The"proper" life time distribution for the same events is given in fig.12.
The lepton charge is assigned on an "a priori" probability defined by the assumed values for Re(x) and Im(x). The dynamics of $K^\circ \to \pi + e + \nu$ decays are those predicted by a pure V-A interaction, taking the form factor f_+=const.

The trajectories of the charged decay products are followed through the magnetic field and their intersection with the wire chambers and counters calculated. Thus the detection efficiency is determined. Numerical results are summarized in Table 2.

As one can see from the quoted values, an efficiency of at least 8% seems easy to obtain in our experiment.

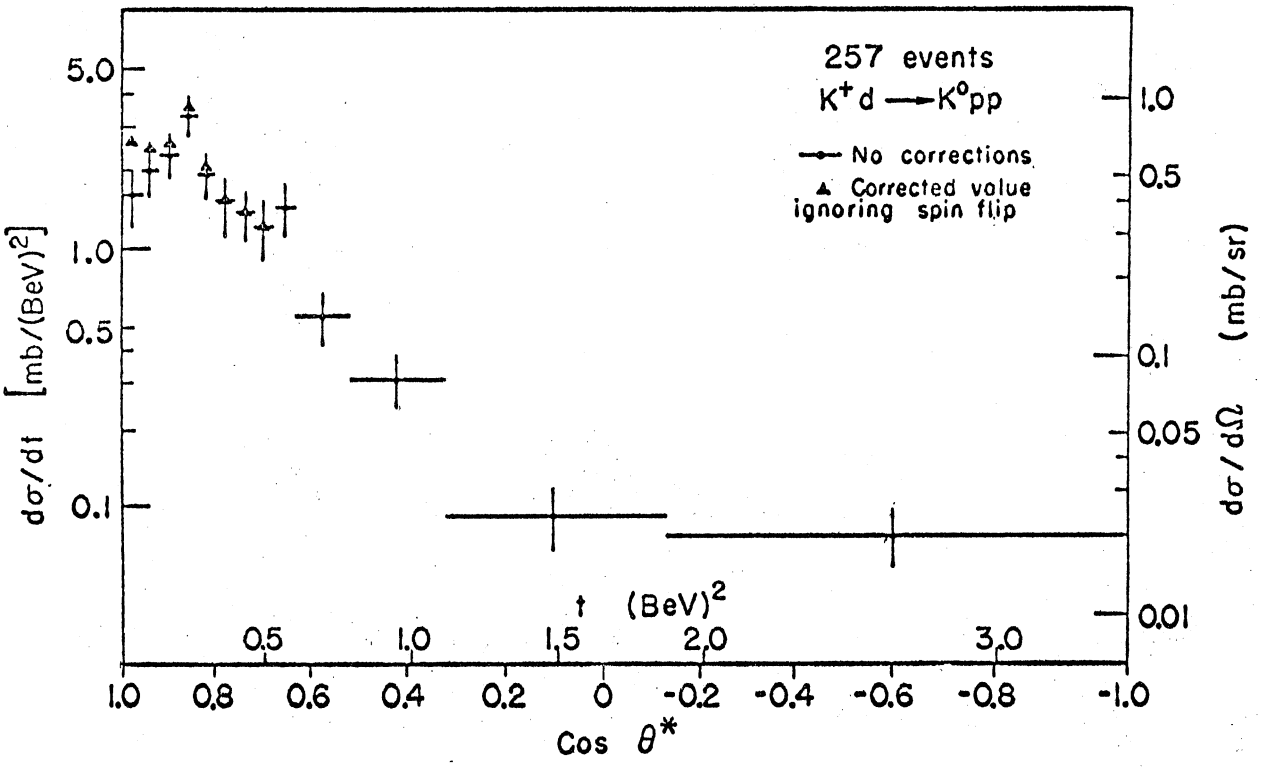

Fig. 8 . C.M. differential cross section (ref. 9).

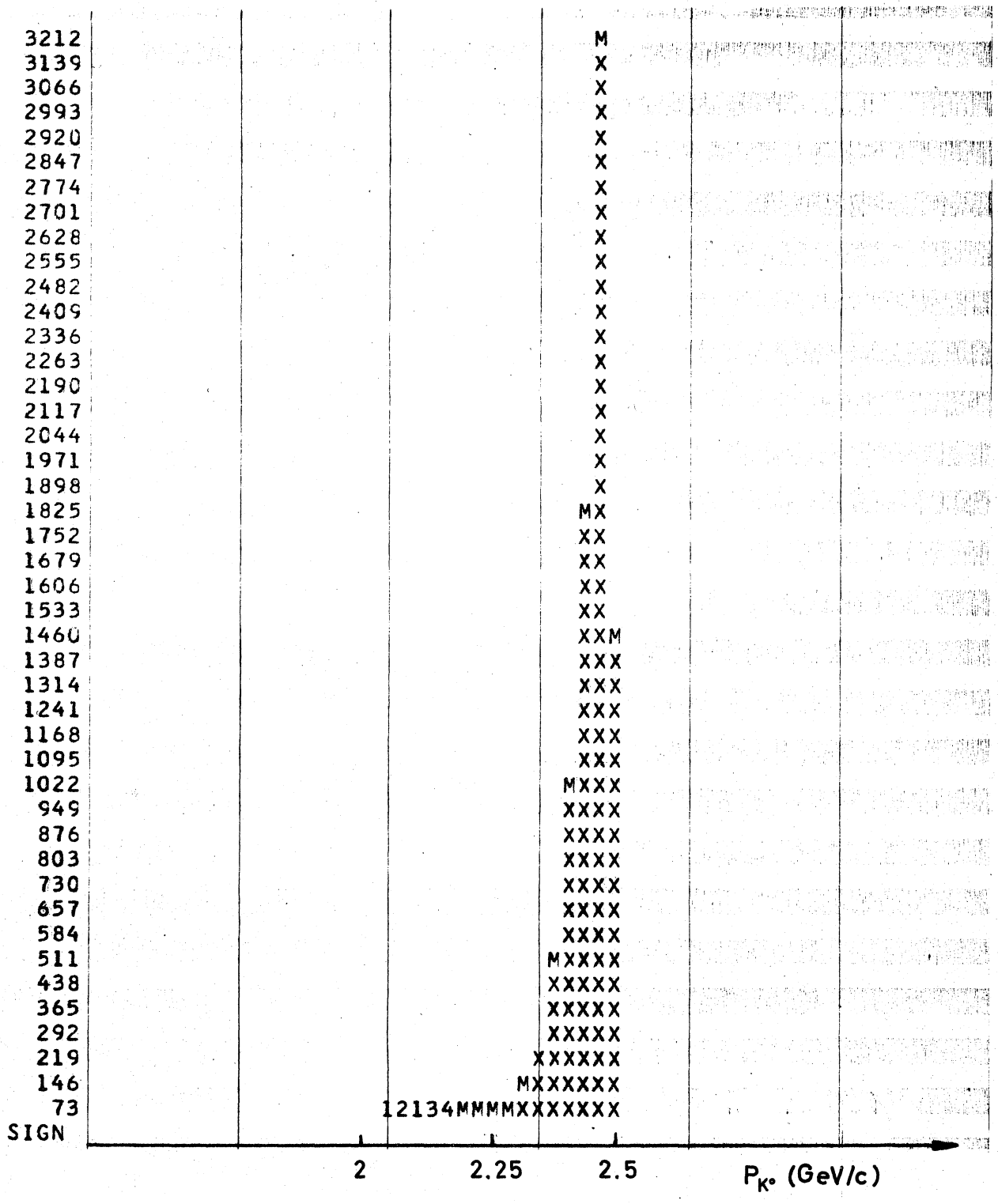

Fig. 9 . Lab momentum distribution of the accepted K° ("elastic" production).

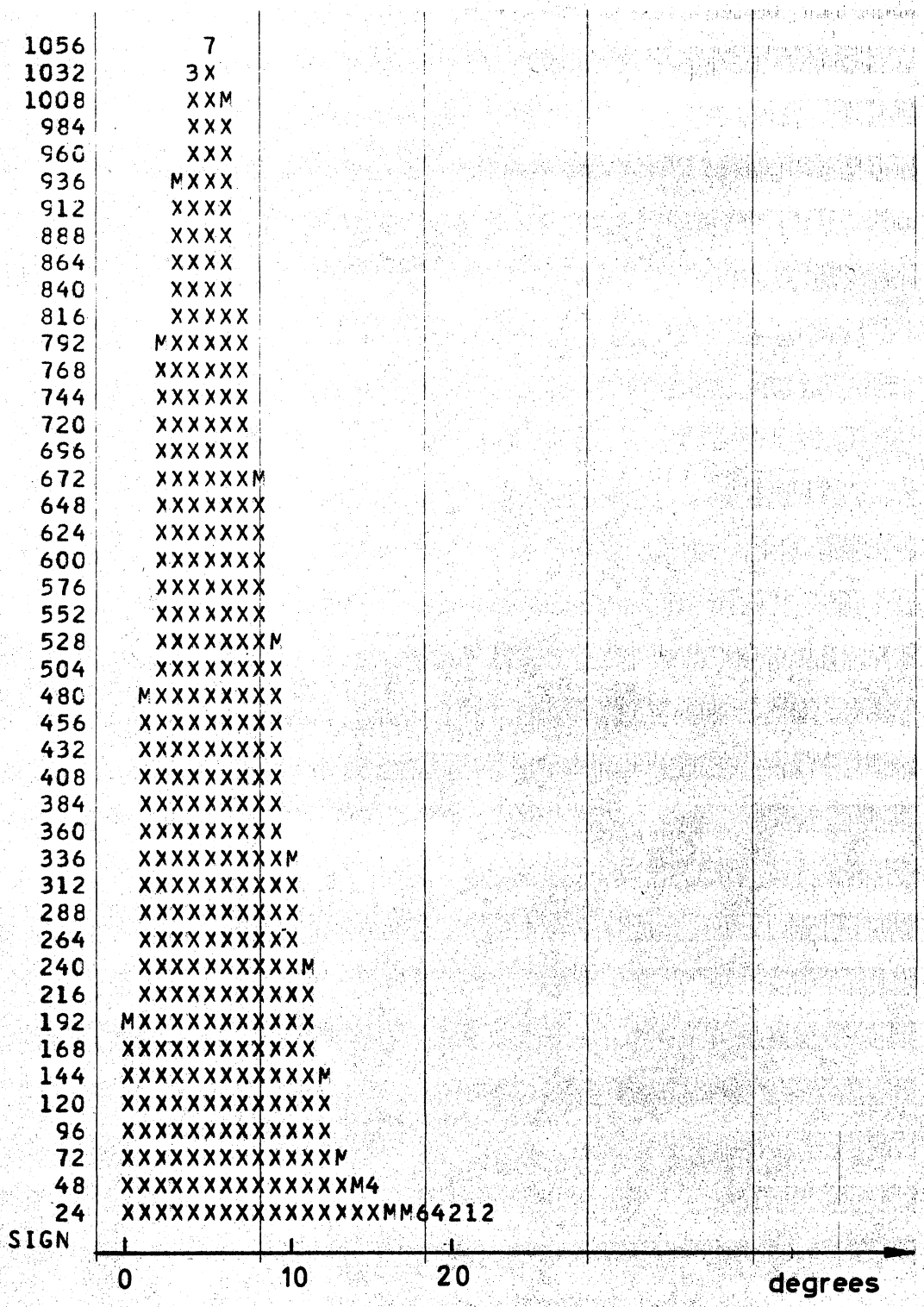

Fig. 10. Laboratory angular distribution of K° accepted by the proposed experimental setup . Only "elastic" charge exchange production is considered.

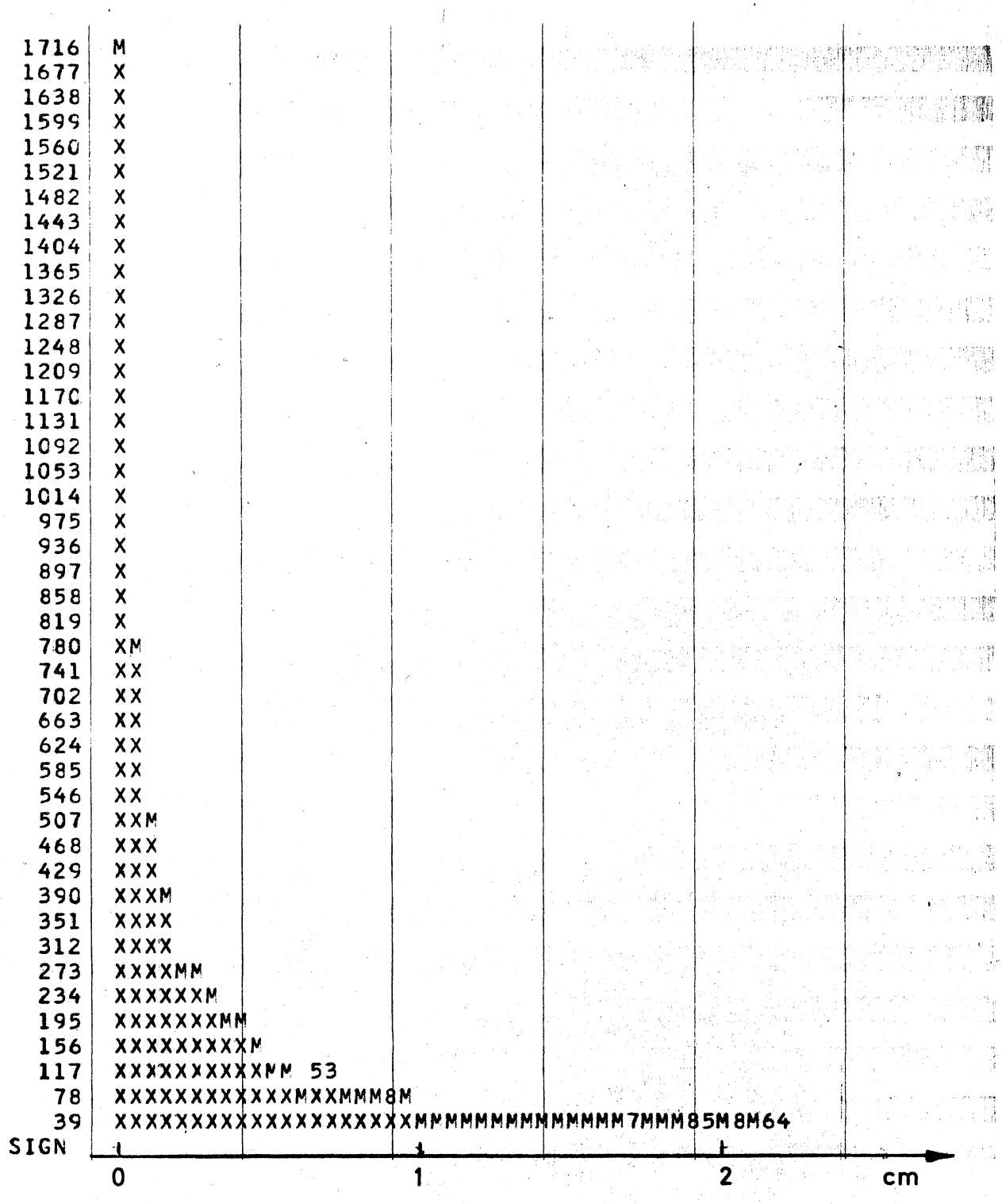

Fig. 11. Range in the Cu target projected along the beam direction of protons emitted in "elastic" charge exchange.

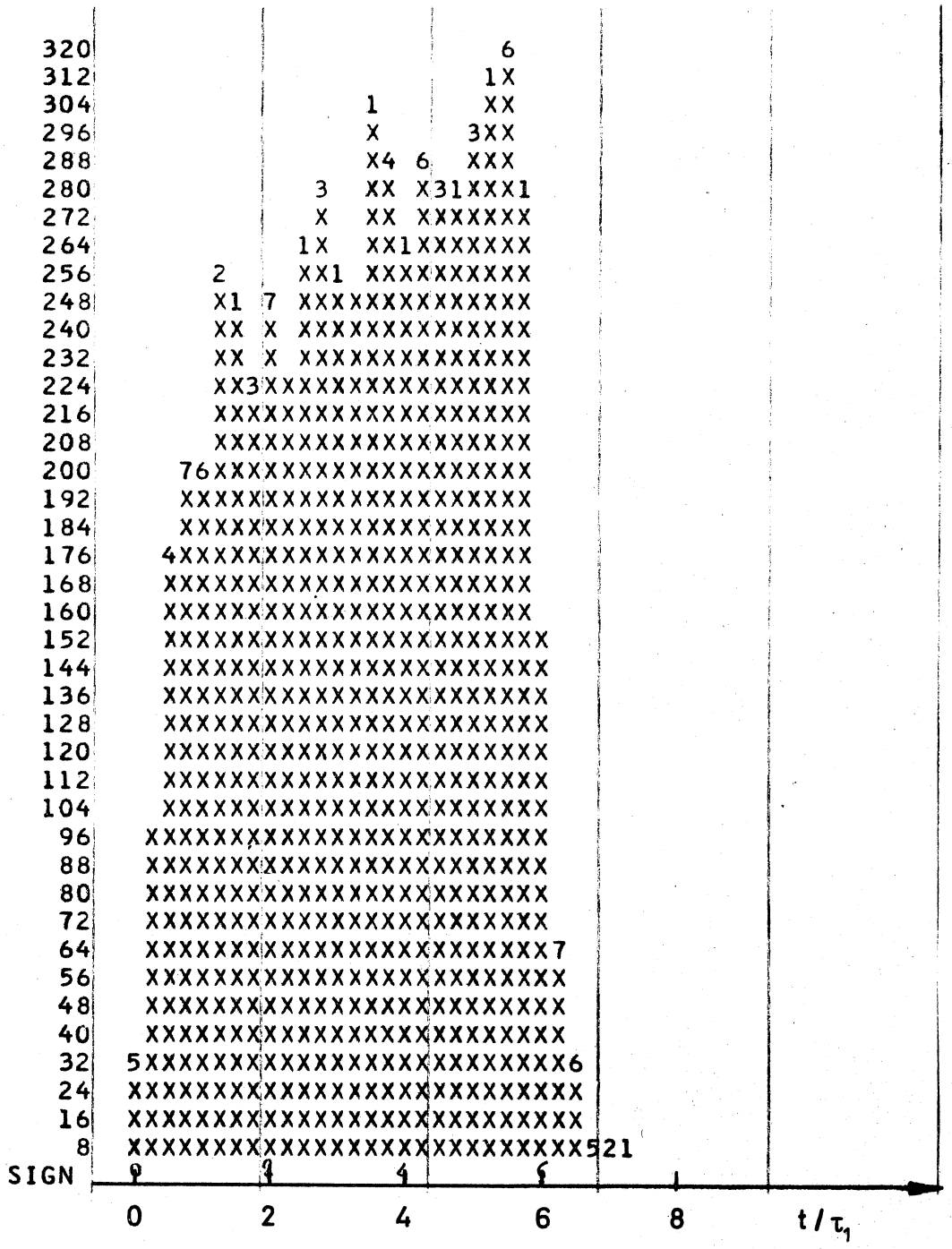

Fig. 12 . K° proper time of flight (in units of K°_1 mean lifetime).

Table 2.

Efficiency of the apparatus

P_{K^+} (GeV/c) =	2.5	3.0	2.5	2.5	2.5
% losses due to: Particles missing the magnet gap	75.5	63	80	75	53
% losses due to: Particles missing the wire chambers	4.5	8.3	1.5	5.2	5.8
% losses due to: π or e missing the Cer.detector	10.	11.7	10	9.8	20
% losses due to: Both charged particles going to the same quadrant of the terminal detec.	2.	5.5	5.1	5.8	8.5
Efficiency	8.0	11.5	3.4	4.2	12.7
Magnet current (A)	200	200	300	200	300
Number of quadrants in the electron detector	4	4	2	2	2

The values in the last column are obtained assuming $\cos \Theta^*_{K^0}$ .94

B. Resolution in "time of flight" determination

Experimental errors

Let us consider the uncertainties on the measured quantities by the reconstruction procedure due to measurement errors.

Having "produced" a number of events, one can simulate the reconstruction starting from the following experimental information: pion and electron coordinates in wire chambers, magnetic field intensity, average coordinates of the production point in the target element, average K^+ direction as defined by the hodoscopes.

A comparison between the "original" and the "reconstructed" values (Fig. 13-22) permits to evaluate the reconstruction errors. Experimental uncertaities taken into account are: in the experation point coordinates $\pm$ .5 cm along the beam direction,due to the target thickness and $\pm$ .25 cm in the normal plane, defined by the hodoscope in front of the target; in the K^+ incident direction $\pm$ .006 rad in the wire chambers coordinate $\pm$ .04 cm (1/3 the wire spacing).

As it appears from the Figs. 14 (a,b,c,d) the uncertainties on the coordinates of the decay point are of the order of: $\pm$ .4 cm along the beam direction pratically constant along the decay volume (Fig. 14a); $\pm$ .1 cm in the normal plane. These values are of comparable magnitude(or less) than the uncertainties at production point.

Let us consider in the errors of the main quantities to be determined, i.e. time of flight and K° momentum, necessary to convert the decay path into proper time. At the K° decay vertex a zero constrint fit gives two possible solutions for K° momentum P'_K and P''_K(Figs. 15a, 15b). Fig. 15a contains "real" events; Fig.15b "reconstructed" events (The enlargement of the regions α, β corresponds to the experimental spread).

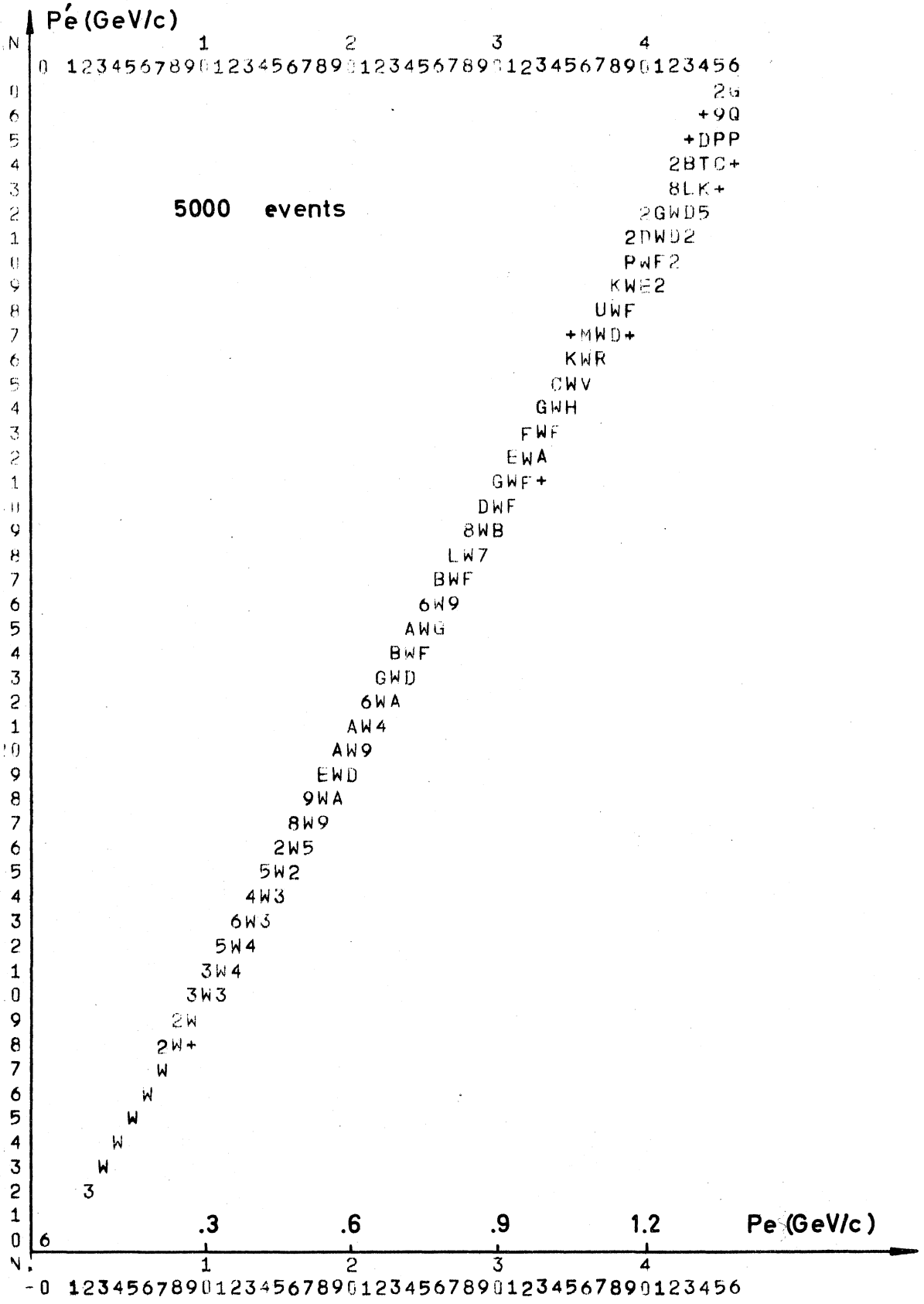

Fig. 13a) Real electron momentum (Pe) Vs reconstructed (Pé).

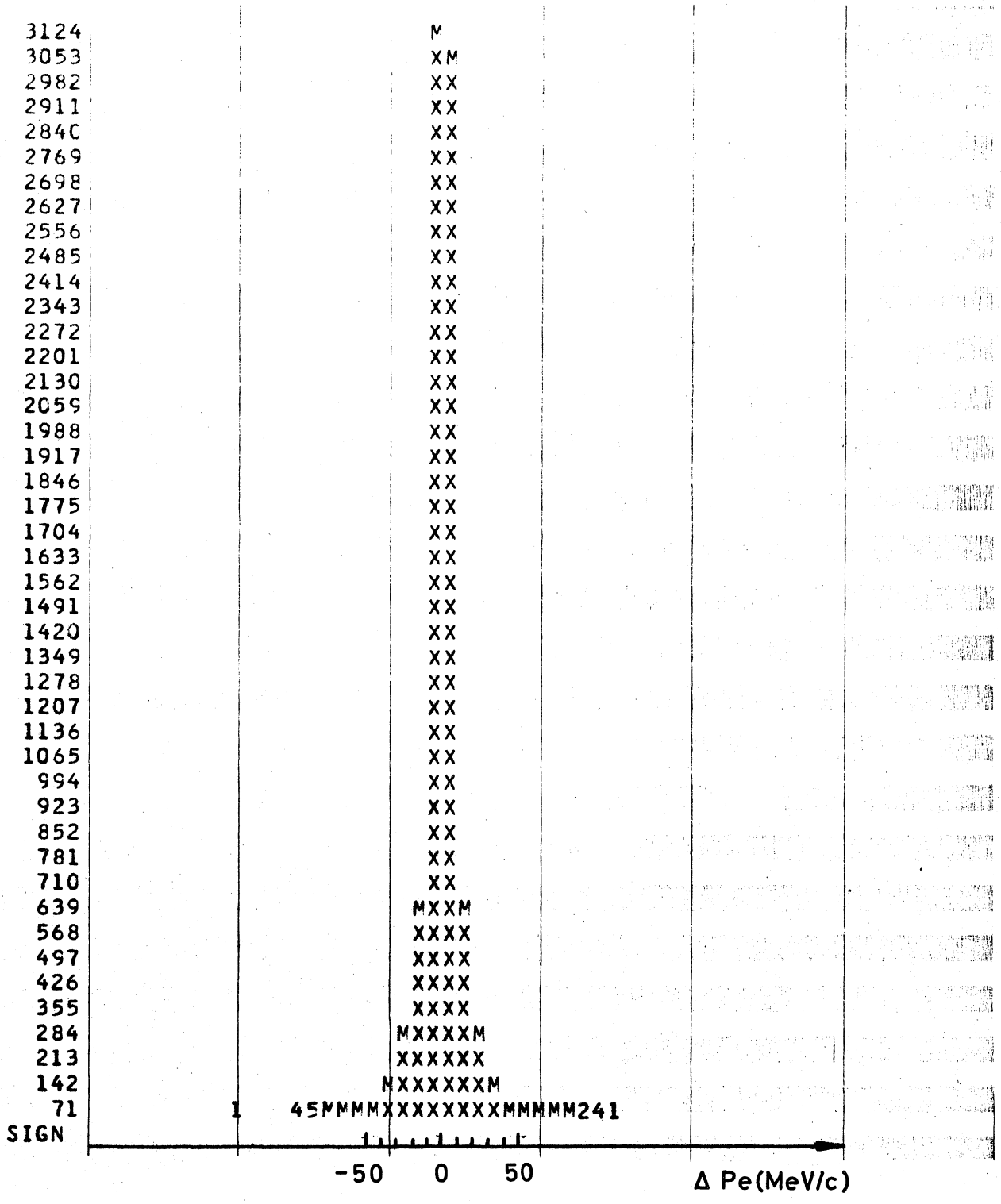

Fig. 13b. Absolute error on electron momentum ($\Delta Pe = Pe - Pe'$).

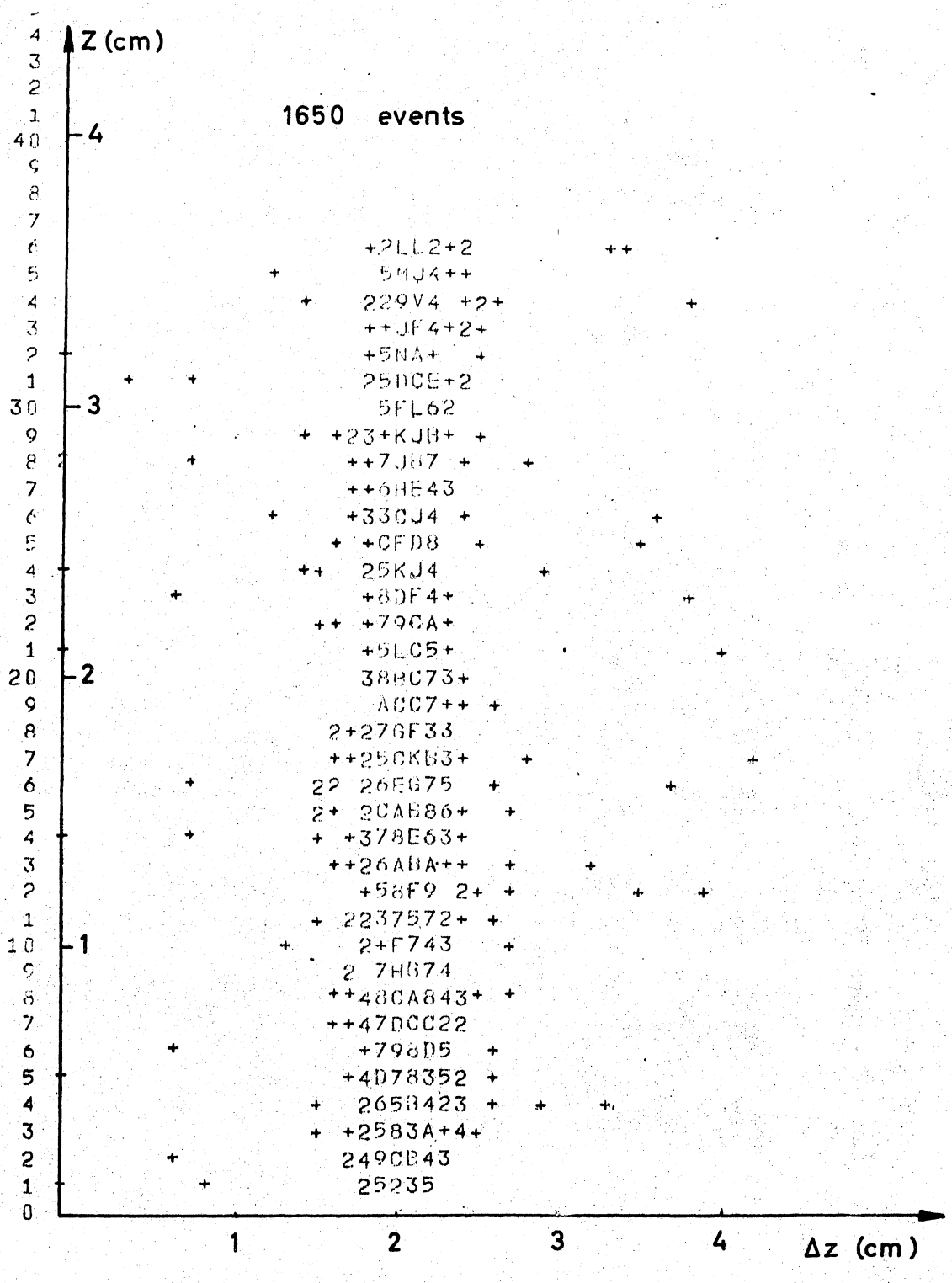

Fig. 14a) $\Delta Z = Z_{real} - Z_{reconstructed}$ of the K° decay points, plotted VS Z coordinate.

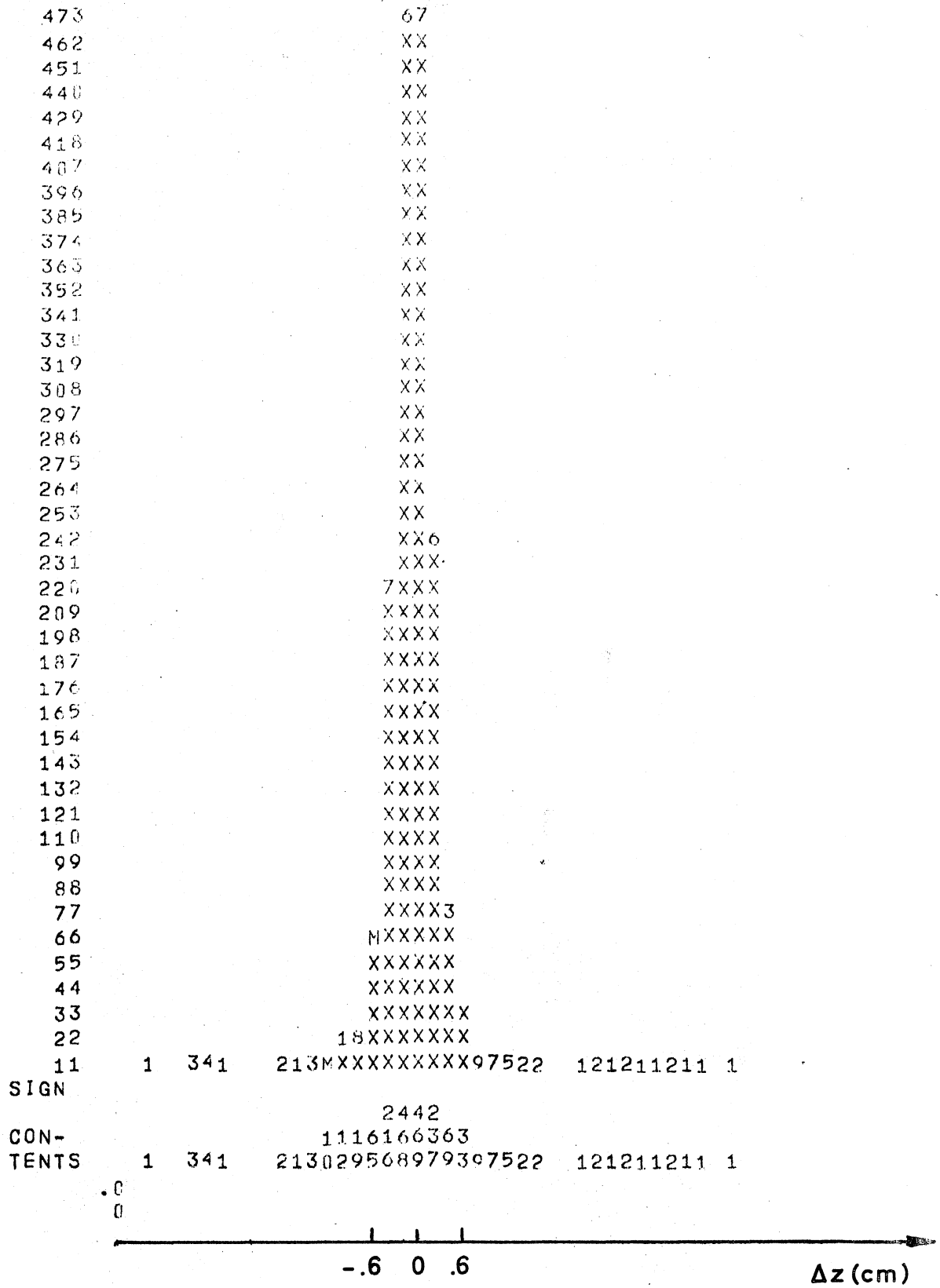

Fig. 14. b) $Z = Z_{real} - Z_{reconst.}$ (half width 4. cm) K° decay point

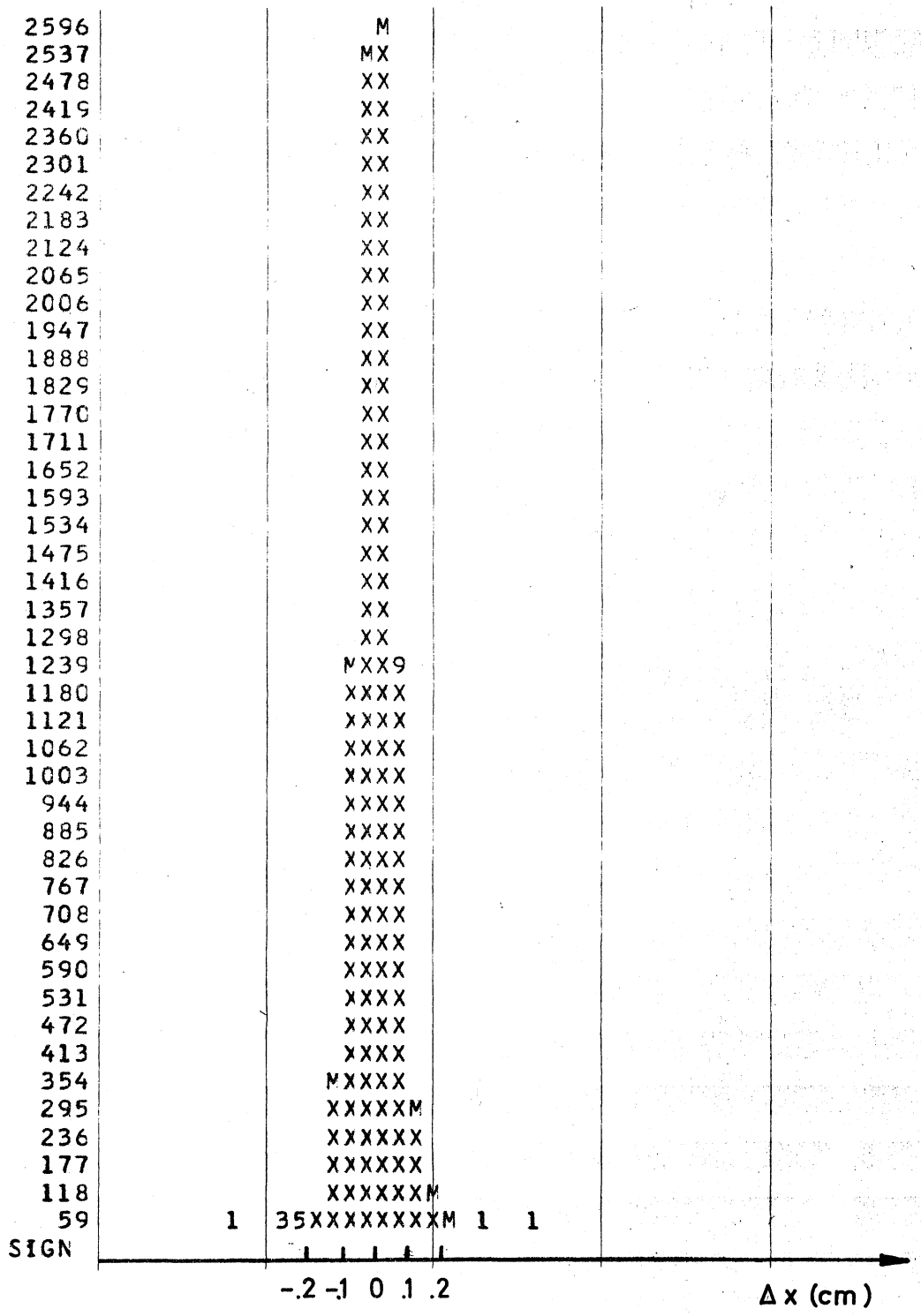

Fig. 14. c) $\Delta x = X_{real} - X_{reconst.}$ (half width $\sim$.05 cm) K° decay point

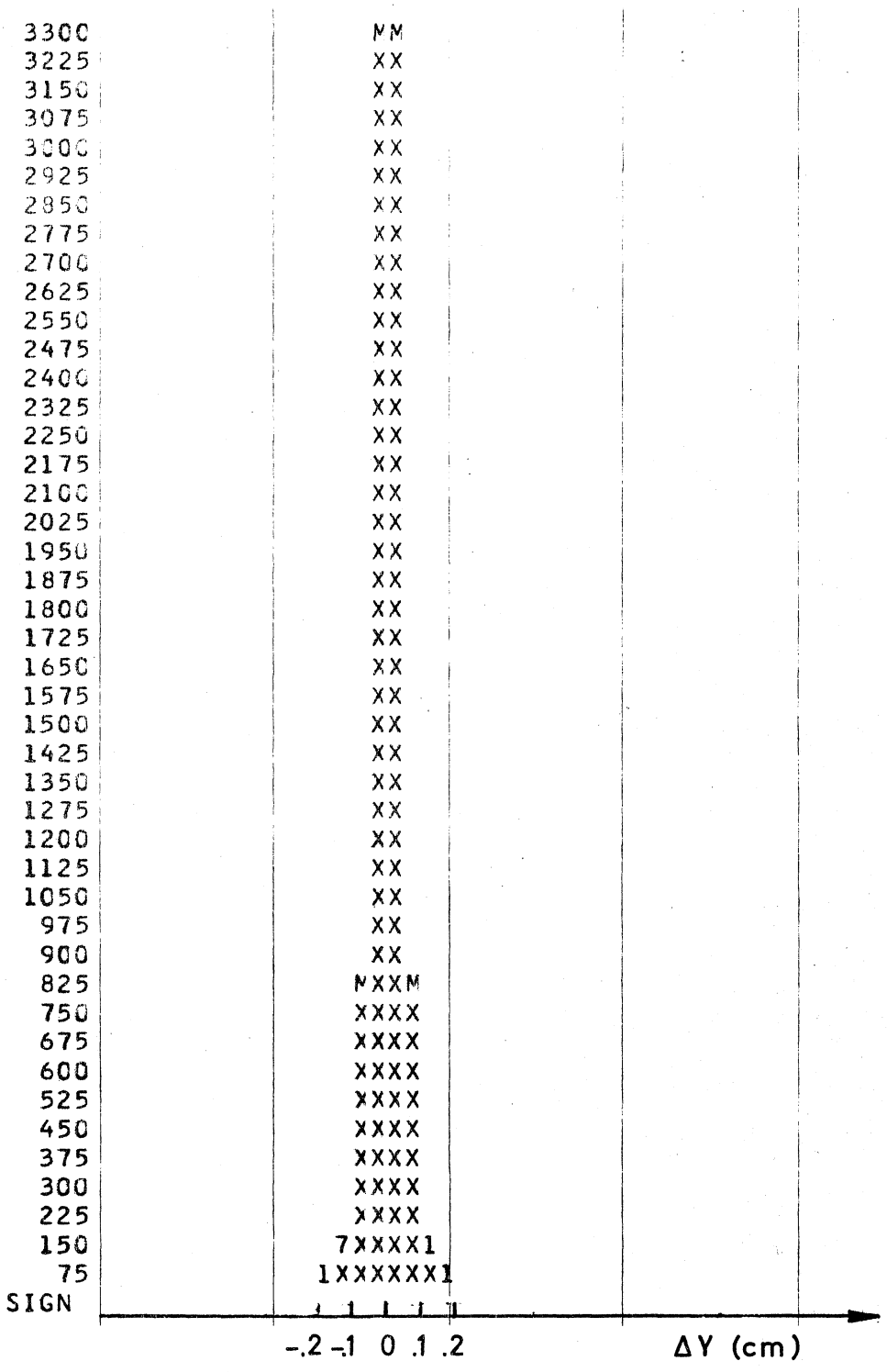

Fig. 14. d) $\Delta y = y_{real} - y_{reconst.}$ (half width $\sim$.05 cm) K° decay point

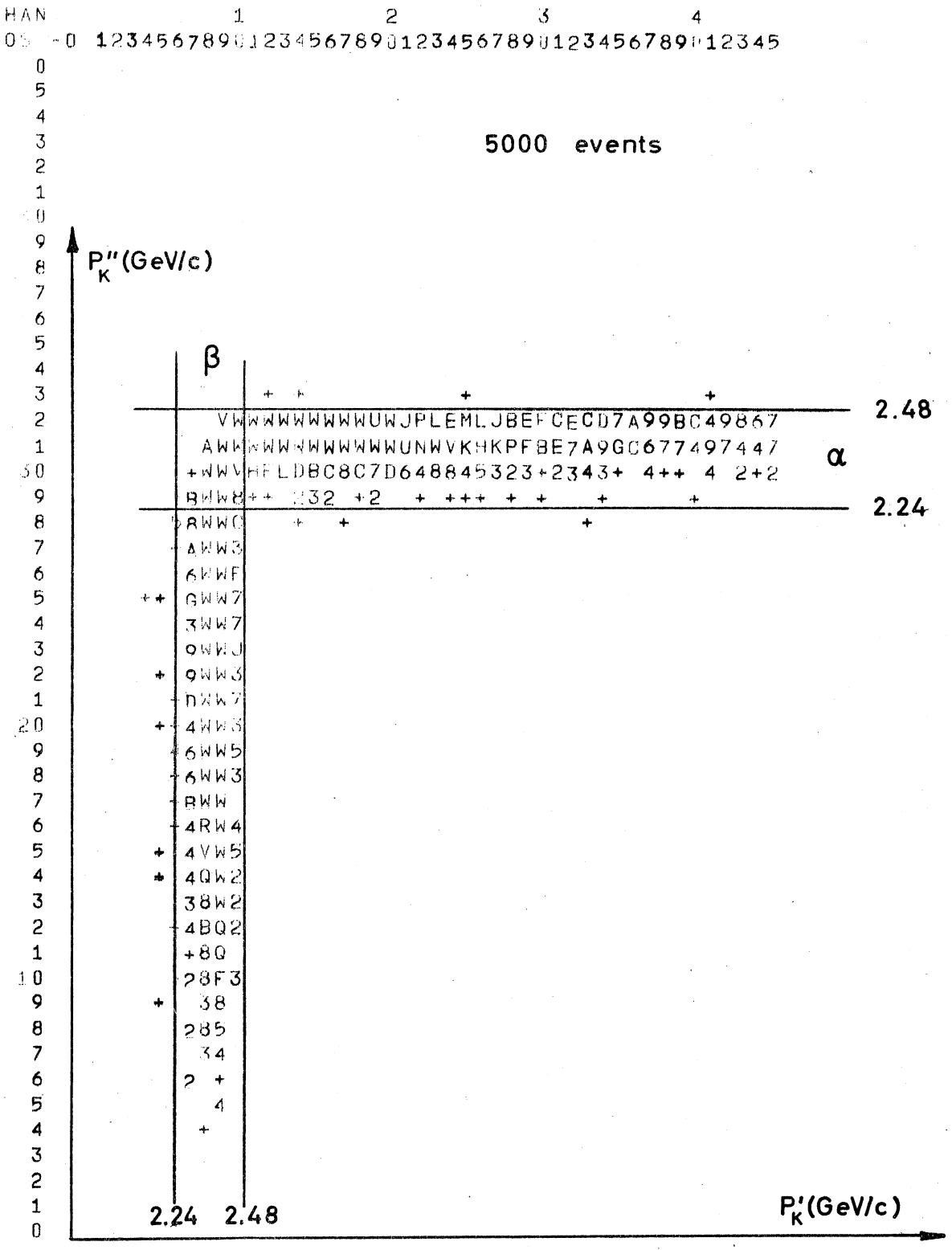

Fig. 15. a) P'_{K° VS P''_{K°. Real events (the two solutions for K° momentum). The width of the regions α and β depends on K^+ momentum and angular spread, target Fermi motion, production angular distribution and geometrica acceptance of the apparatus.

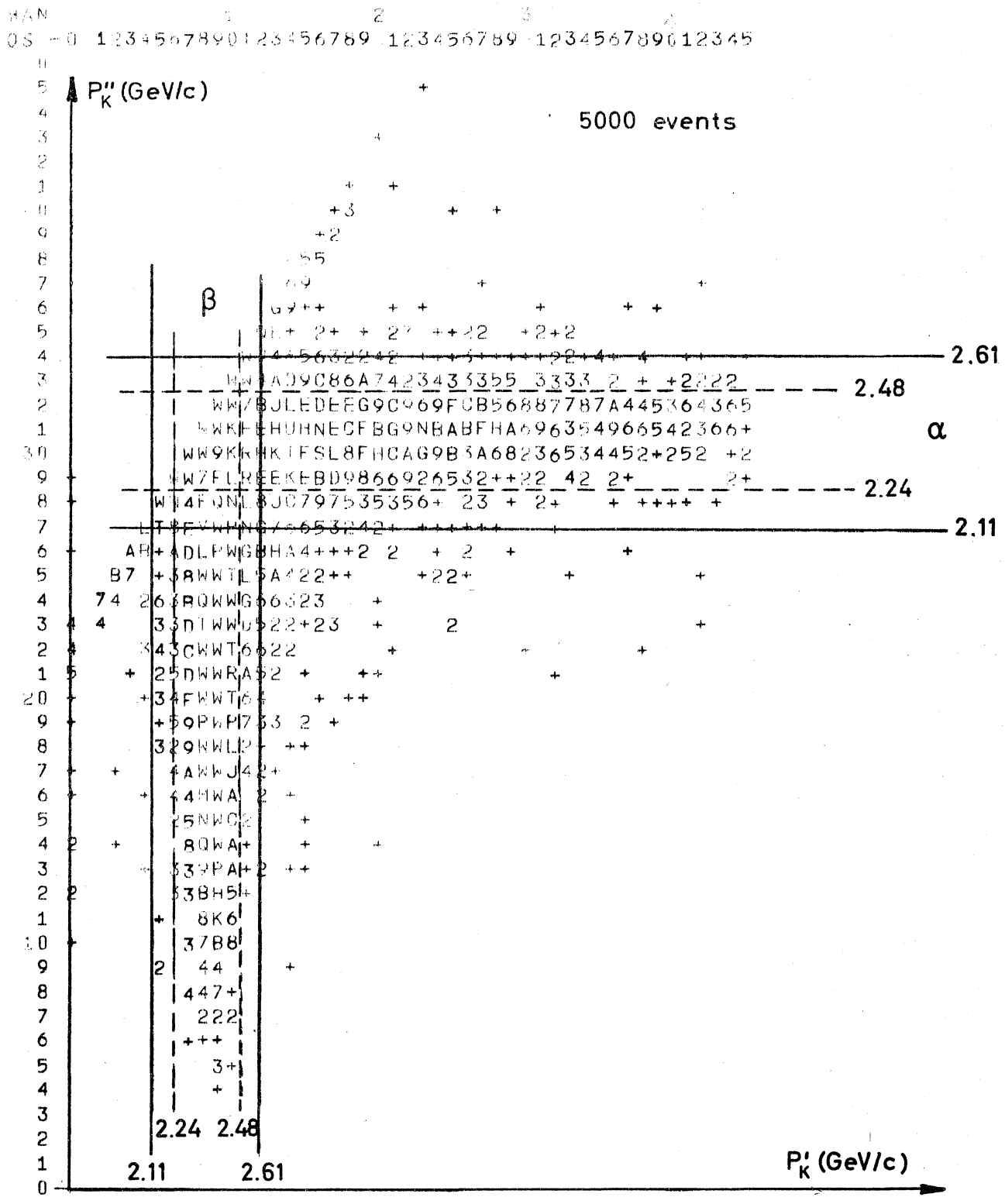

Fig. 15. b) P'_{K° VS P''_{K°. Reconstructed events. The resulting width for regions α and β is the original width (dotted lines, from fig. 15a) increased by experimental errors. Region α contains acceptable events.

The following cases are possible:

α) one of the solutions gives a value which is higher than the maximum momentum $\bar{P}_{K^\circ}$ compatible with the angle of emission. In fig.15a this case is represented by points in region α .

β) both solutions are acceptable, i.e. both $\leq \bar{P}_{K^\circ}$. These points are represented in region β . Smaller values could be due to K°'s produced inelastically.

When this happens, there is no way to decide which is the true solution, and one is forced to disregard this kind of events ($\sim$ 40% of the total sample of recorded events). In fact inelastic charge exchange can take place in any of the following processes

$$
\begin{aligned}
K^+ + (p) &\longrightarrow K^{*+} + p \\
&\qquad \big\lfloor \longrightarrow K^\circ + \pi^+ + p \\
&\longrightarrow N^{*++} + K^\circ \\
&\longrightarrow \pi^+ + p + K^\circ \\
K^+ + (n) &\longrightarrow K^{*\circ} + p \\
&\qquad \big\lfloor \longrightarrow K^\circ + \pi^\circ \\
&\longrightarrow K^\circ + N^{*+} \\
&\longrightarrow K^\circ + p + \pi^\circ \\
&\longrightarrow K^\circ + n + \pi^+
\end{aligned}
$$

which have a cross section comparable with the "elastic" processes (4.1).

Of the above processes, the most important one is that associated with N^* and K^* production. Due to the lack of precise experimental knowledge a simple model has been used, assuming that in the C.M. frame the angular distribution of the N^* is the same as that of the recoil nucleon in elastic production processes and, moreover, that the N^* decay isotropically in teir rest system.

Proceeding as for the elastic events, one can calculate the solutions one obtains from the "reconstruction" of inelastic ones. The scatter diagram is shown in fig.16. In about 25% of the inelastic events produced by this channel (N^*) the analysis would determine the momentum in an unambigous way.

Similarly for K°'s from K^* production. The acceptance, in this case is reduced to $\sim$10%. Similar percentage is obtained for the contribution of all other non resonant channels.

In total, the sample of events accepted in the "reconstruction analysis" contains 40% of the elastic production and $\sim$40% of the inelastic.

In fig. 17 - 18 the difference $\Delta \underline{P}$, between the true K° momentum for "elastic " events and the "experimental" K° momentum $\underline{P}_K$ reconstructed starting from decay parameters and average production for region A, is plotted vs decay position along the beam. Half width in the $\Delta \underline{P}$ distributions, roughly indipendent of Z coordinate in the decay volume, is about 130 MeV/c. This value, that takes into account all the reconstruction errors, corresponds to $\sim$5% of the K° mean momentum, selected by our apparatus. The figs. 19-20, corresponding to the preceding ones, represents $\Delta P'$ distribution for all events, in the hypothesis of "elastically" produced events. In this case "experimental" K° momentum is calculated only by production kinematics, ignoring all decay parameters, except decay point. The resulting error is $\sim$3% of the K° mean momentum. Finally it may be worth noting that one could use this value for the K° momentum in the case of complete separation between "elastic" and inelastic events. This separation depends mainly on the two-body production angular distribution and measuring errors.

With the assumed angular distribution and the above

momentum resolution only a fraction of "elastic" events can be unambiguously reconstructed. These events will constitute a reduced, but very precise sample for the final analysis.

In analogous way fig. 21 is the error $(\frac{\Delta T}{\tau})$ distribution of the K^o time of flight, in units of the K^o_1 mean lifetime. ΔT is again defined as the difference between real and reconstructed (from P_{K^o}) values $\Delta T = t_{real} - t_{recon}$. The width of the distribution, $\sim 7\%$, results indipendent from the time of flight (fig. 22) so insuring a very good time resolution in all the time interval (~ 6 K^o_1 lifetimes).

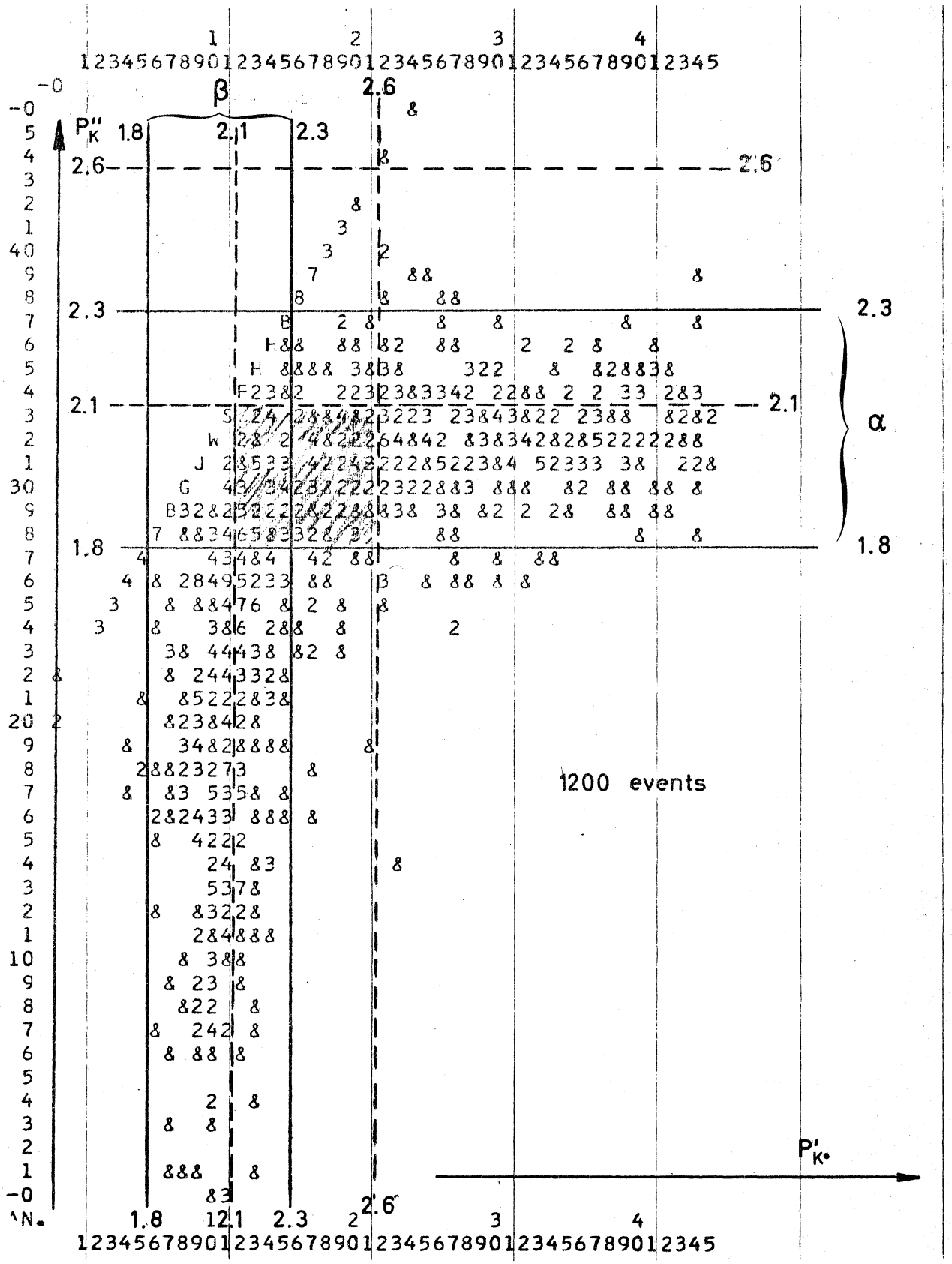

Fig. 16. P'_{K° VS P''_{K° . (reconstructed anelastic events: $K^\circ N^*$). The regions between the dotted lines contain the "elastic" events. Consequently, events in the shadowed area are to be rejected. Useful events correspond to points in the remaining region .

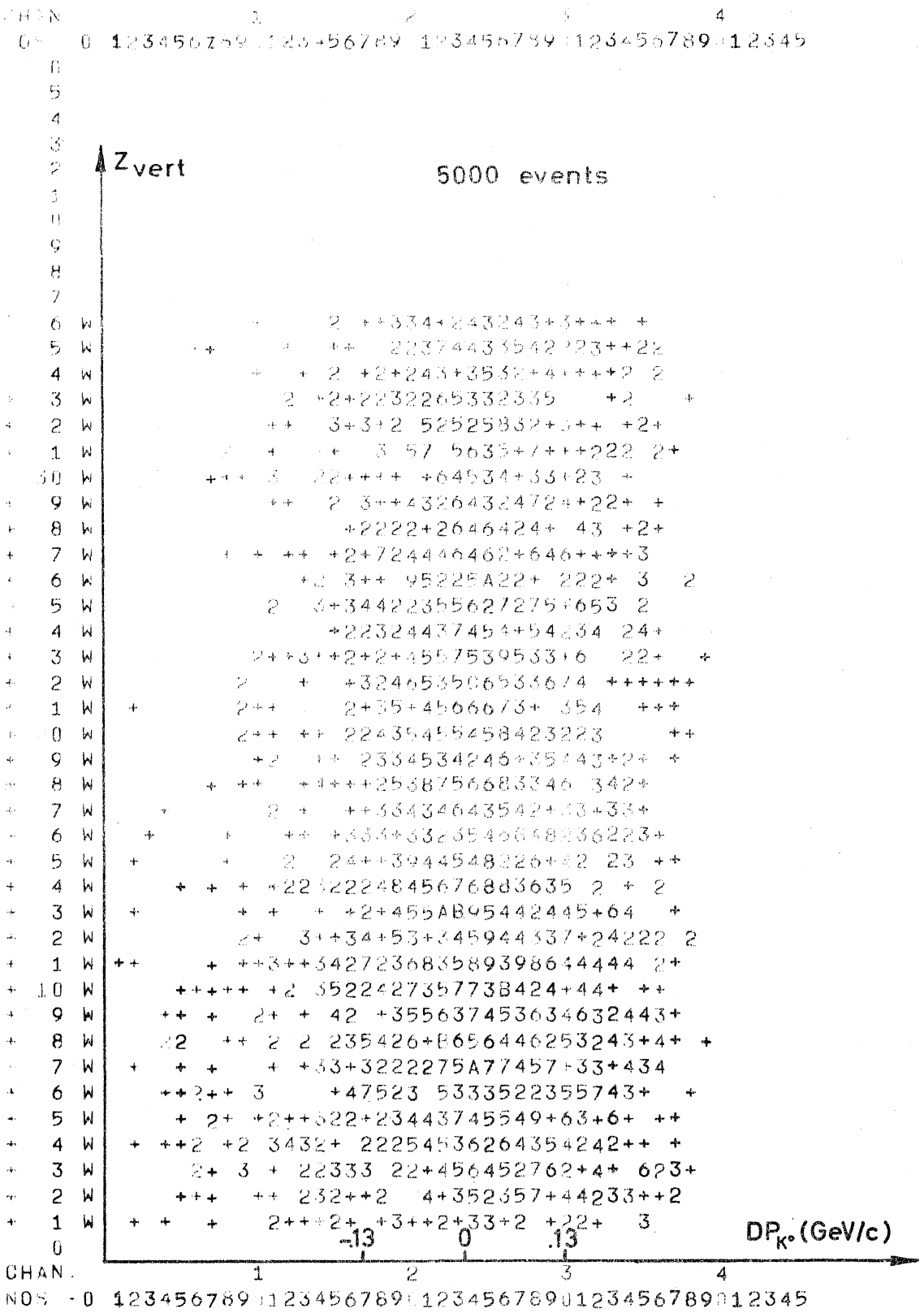

Fig. 17. $DP_{K^\circ} = P_{K^\circ real} - P''_{K^\circ reconst.}$ VS Z VERTEX (Z coord. of decay point)

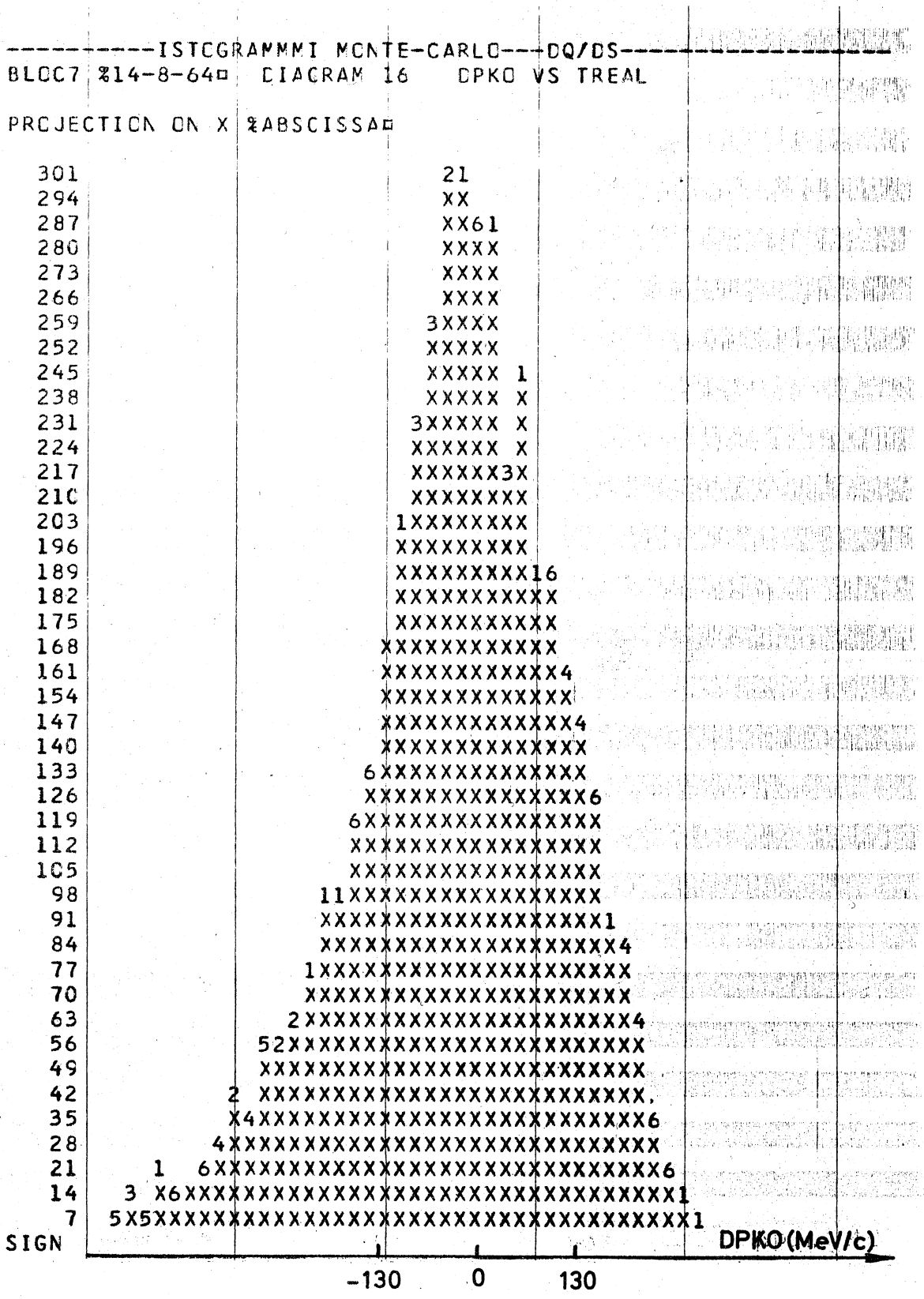

Fig. 18. DP_{K° distribution

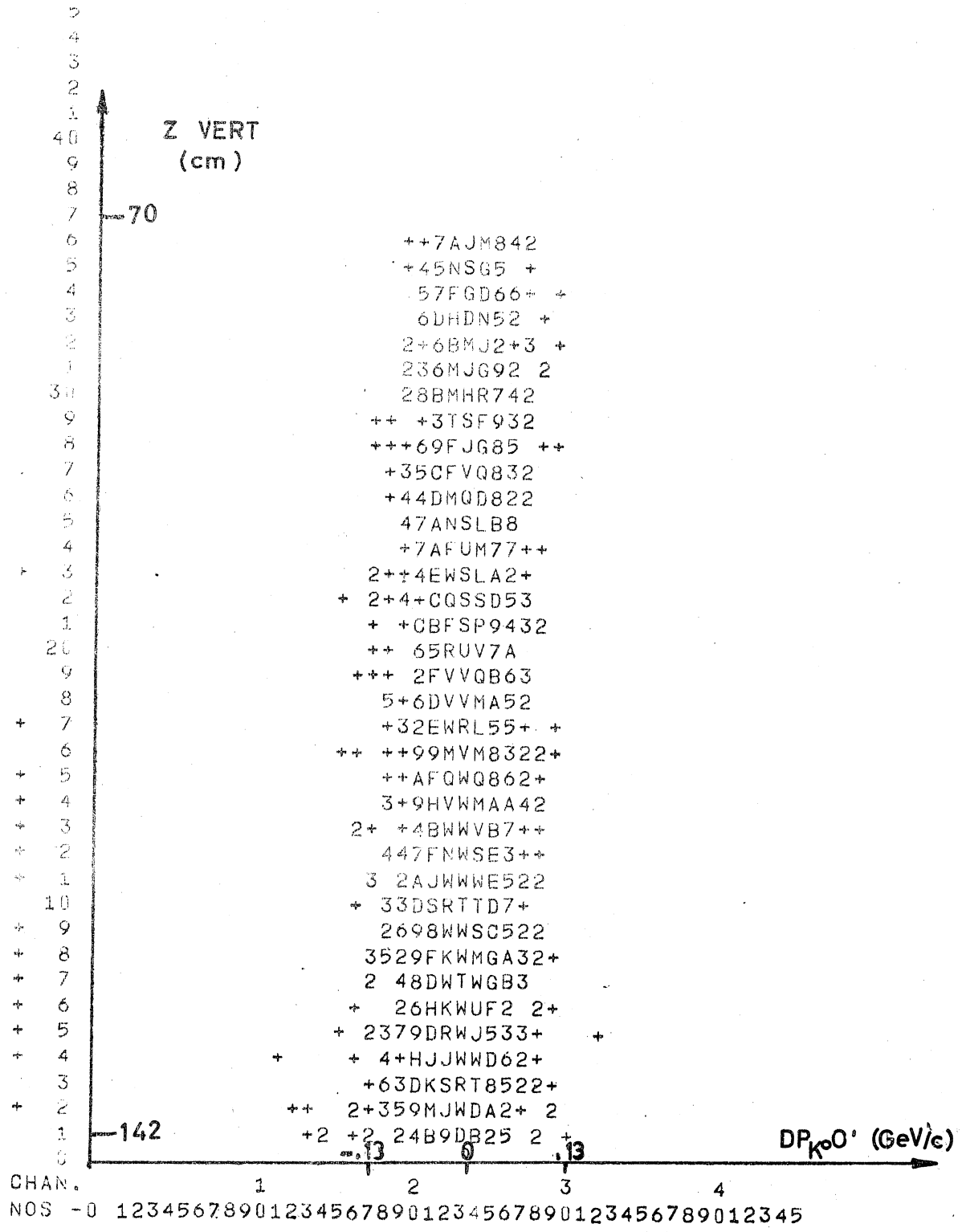

Fig. 19. $DP'_{K^\circ} = P_{K^\circ real} - P_{K^\circ "elast."}$ VS Z vertex

$P_{K^\circ "elast"}$.. is obtained, in the hypotesis of "elastic" reaction, with average values for production kinematics parameters.

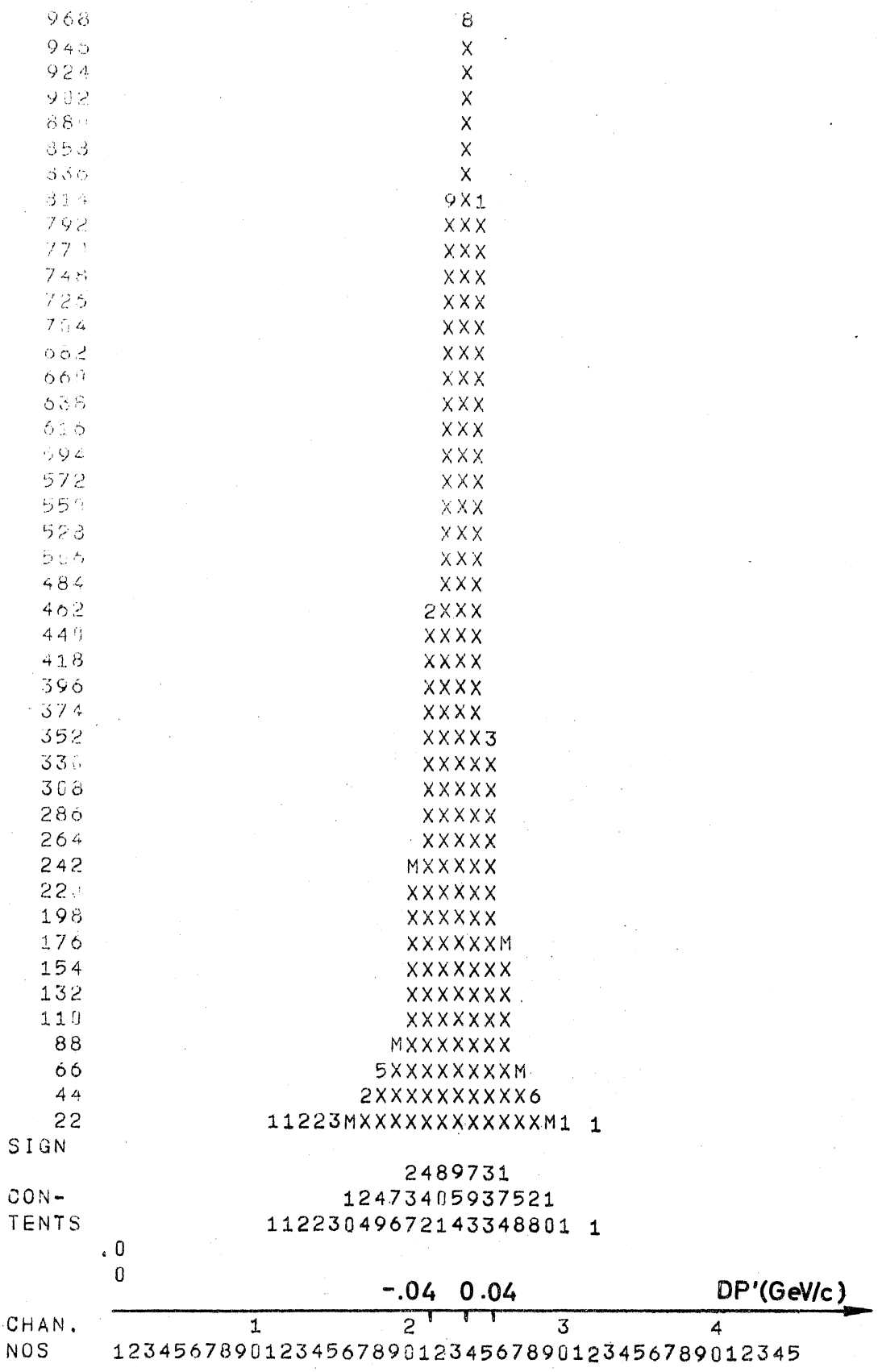

Fig. 20. DP'_{K^0} distribution

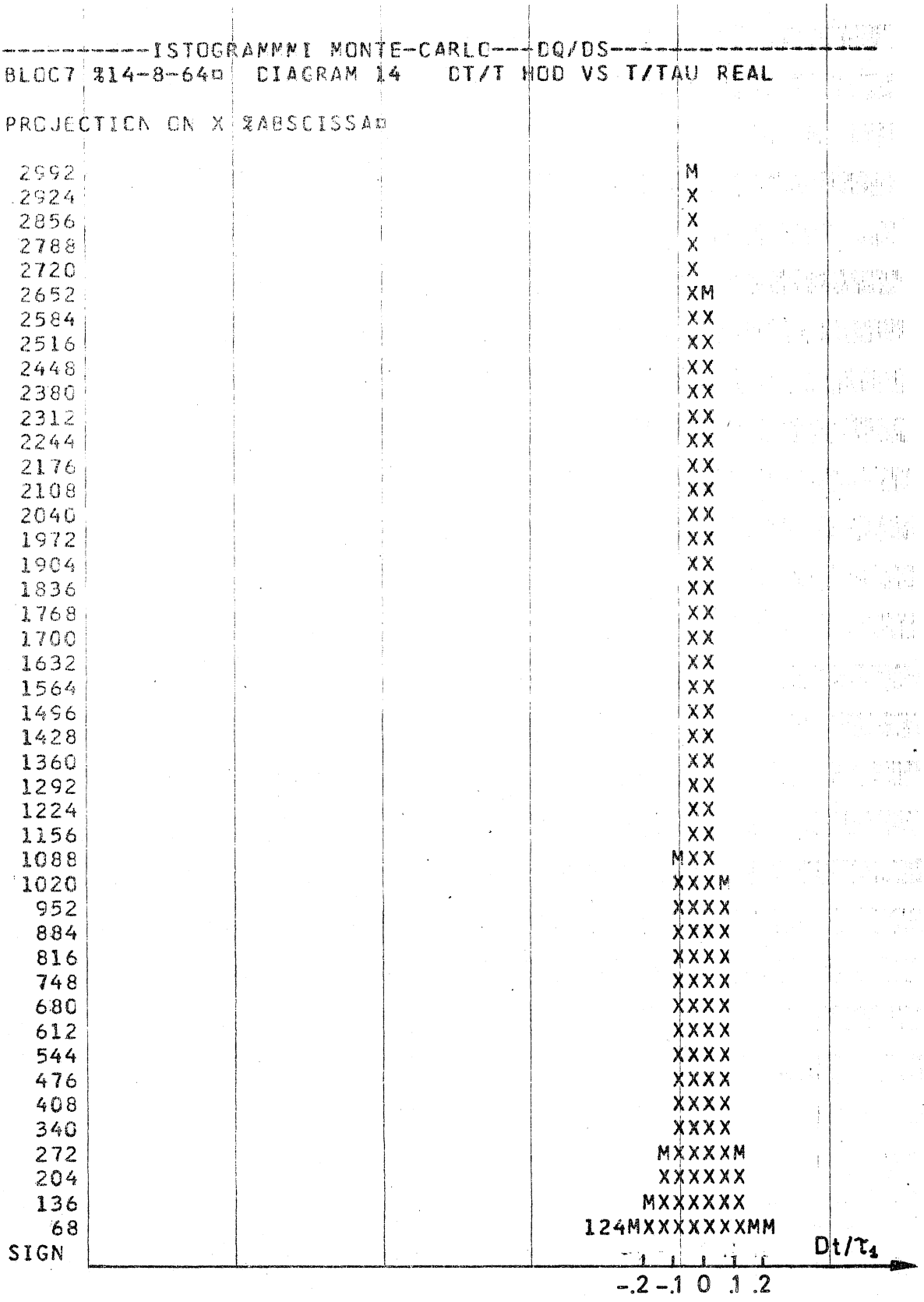

Fig. 21. $(t_{real} - t_{reconst.})/\tau_{K^0_1}$. Proper time error. $t_{reconst.}$ is the time of flight computed from the value of K° momentum chosen at decay point (solution P''_{K^0})

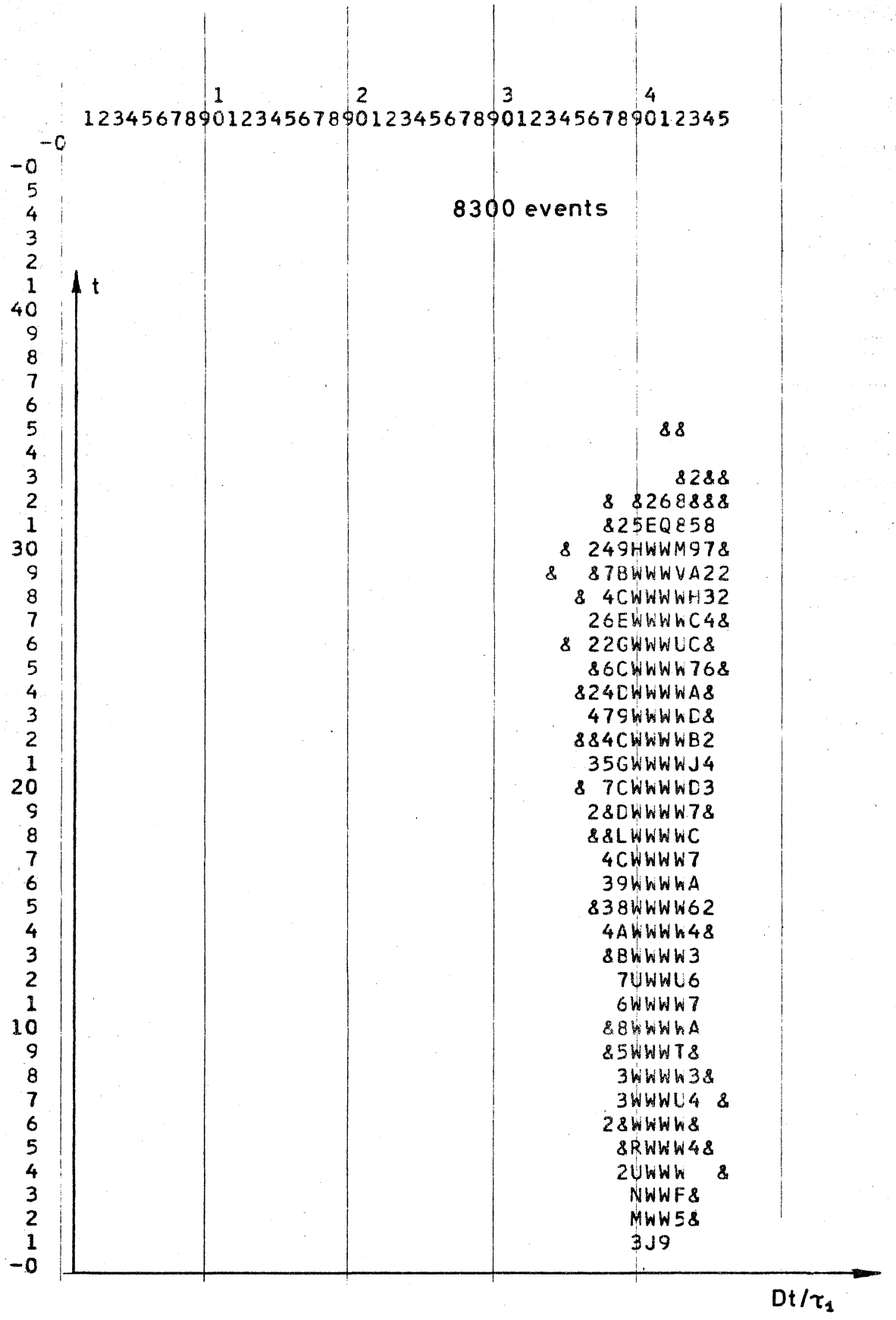

Fig. 22. $(t_{real} - t_{reconst.})/\tau_{K^0_L}$ VS $t_{real}/\tau_{K^0_L}$

C. Background.

We have to deal mainly with two different types of background.

1) K^o anelastically produced: wrong momentum may be assigned outside the accepted region. As discussed in the preceding section, with appropriate K^o momentum cutoff; a negligible fraction of wrong momentum K^o will survive in the final sample.

2) Events simulating K^o_β decay.

- $\gamma \rightarrow e^+ + e^-$

The requirement of only one minimum ionizing track in the electron detector will considerably reduce the trigger due to electron pairs. In any case from the final sample will be rejected all events giving a missing mass less than 70 MeV if interpreted as electron pairs. No background event will survive and the loss of good events will be about 2% (fig. 23).

- $K^o \rightarrow \pi^+ \pi^-$ triggering the gas Čerenkov counter. The Čerenkov feed-through is $\sim .5\ 10^{-3}$. A missing mass cutoff (resolution $\simeq$ 3 MeV) will eliminate this source of background, rejecting the events giving a missing mass = 498 ± 12 MeV (4 standard deviations) from K^o mass). The loss of K^o events falling in this interval, is $\leq$ 10% (fig. 23).

- $K^o \rightarrow \pi^+ \pi^- \gamma$ with γ conversion in the electron detector wall and scintillators. Due to the small amount of traversed material (conversion probability $\sim$<1%) and to the small $K^o \rightarrow \pi \pi \gamma$ branching ratio ($<$ .3%) [12], [13], we can conclude that this type of background will be less 0.1%, even disregarding the geometrical efficiency factor.

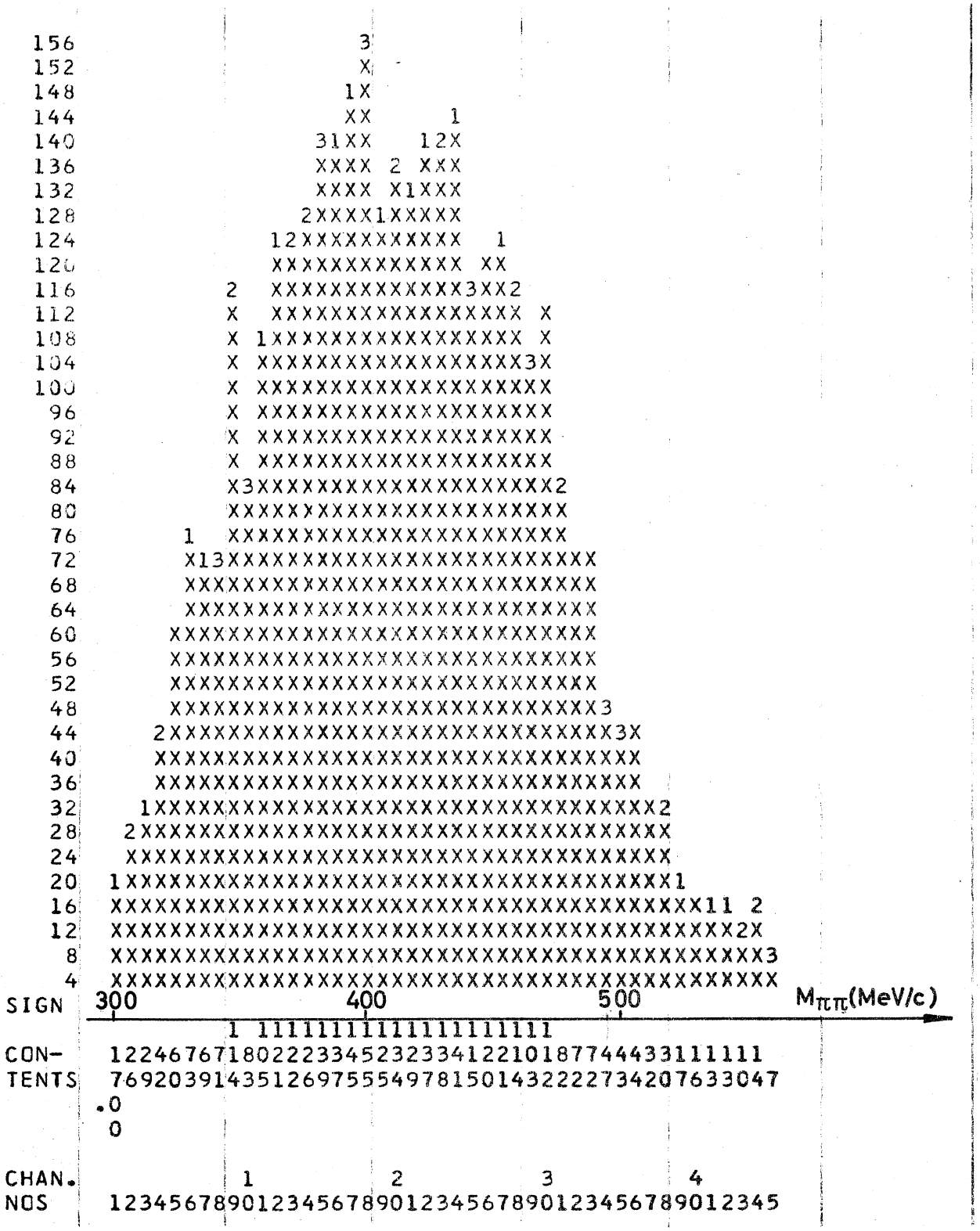

Fig. 23. $M_{\pi\pi}$ Missing mass of the 2 charged decay products in $\pi - \pi$ assumption.

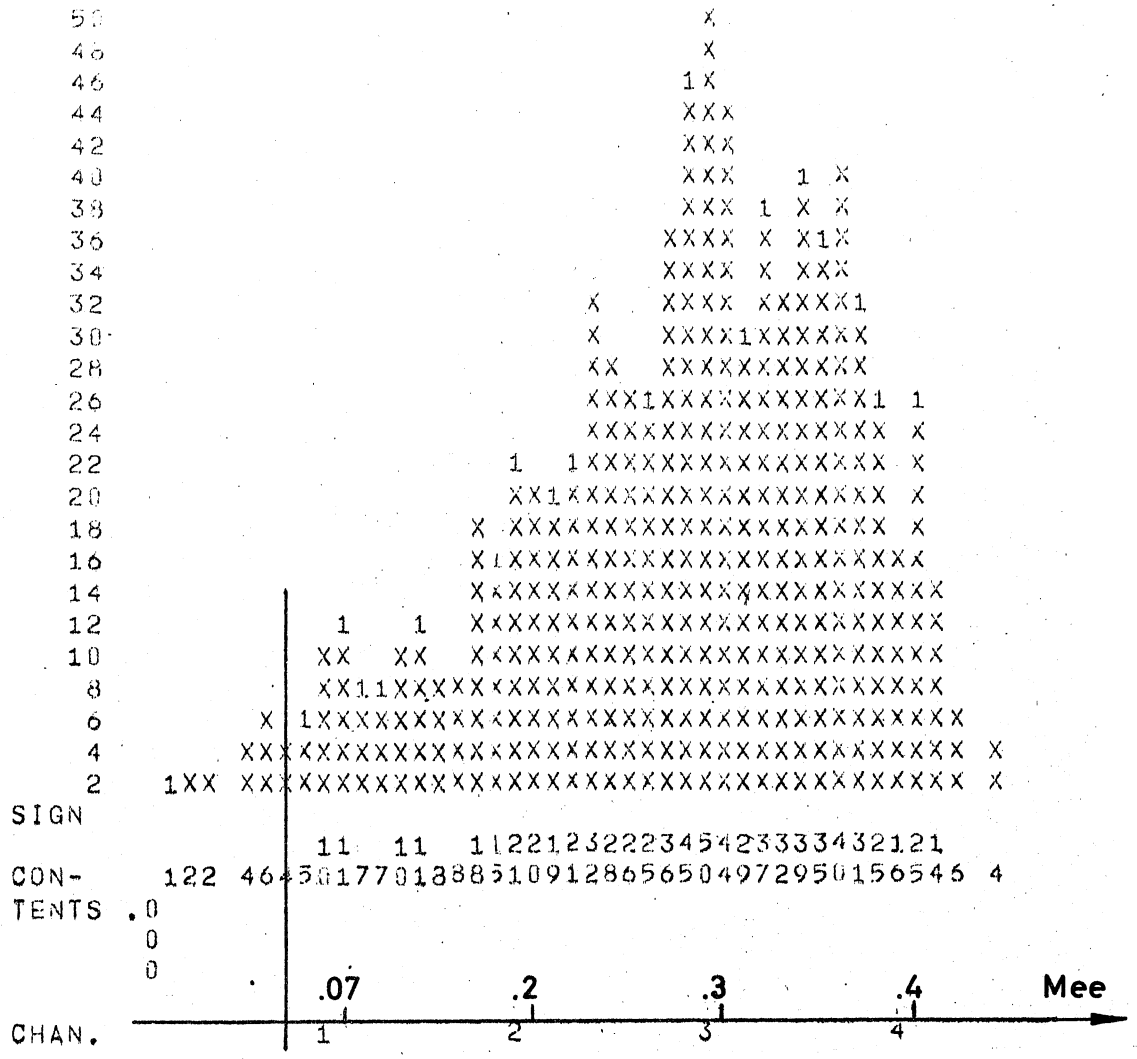

Fig. 24. M_{ee}. Missing mass of the 2 charged decay products in e-e hypotesis.

- $K^0 \rightarrow \pi^+ \pi^- \pi^0$

With similar considerations as before one can evaluate to few $^0/_{00}$ the contribution to the background from this decay. This value has to be further reduced for geometry requirements (one electron has to cross the final Cerenkov in $\pm$ 20°).

Decay and production fit (see, for instance, discussion of references 13) may also help in rejecting these events.

- $\Lambda^0 \rightarrow p\ e^- \bar{\nu}$

This type of events might constitute a serious trouble in our experiment, because it simulates events of the forbidden type $K^0 \rightarrow \pi^+ e^- \nu$ in the first lifetimes. Nevertheless, the effect is negligible, because Λ^0 are produced mainly via $\pi^+ N \rightarrow K^+ \Lambda^0$ (cross section of the order of .5 mb) and

a) the rejection efficiency against pions of the Cerenkov counters on the beam is of the order of 99.9%;

b) the production angular distribution favours K^+ in the forward cone, controlled by the anticoincidence;

c) Λ_β decay has a rate 10^{-3} less than the normal mode.

D. Events rate.

To evaluate the counting rate of our apparatus, we have to make some assumptions about the cross section for the "elastic" charge exchange reaction

$$K^+ (N) \rightarrow K^o P$$

By using the cross section measured in deuterium, a Fermi gas model for the Cu nucleus and taking into account the Pauli principle the total charge exchange cross section results $\sim$ 12 mbarns/Cu nucleus. This figure corresponds to an interaction mean free path in Cu of $\sim$ 1000 cm.
With the following input parameters:

beam intensity 10^5 K^+ /pulse

beam momentum $2.5 \pm .05$ GeV/c

geometrical average detection efficiency .08

loss for ambiguous P_{K^o} solutions and background cutoff .05

target thickness Cu 5 cm

decay length 80 cm (.009 K_2^o lifetimes $\sim$ 6 K_1^o lifetimes)

$K_{2\beta}^o / K_2^o$ branching ratio .38

electron detector efficiency $\sim$ .9

the resulting rate is of the order of .06/pulse accepted K_2^o, produced by charge exchange K^+ "elastic" interactions.

On the other hand, a fraction of K^o produced by anelastic processes will also trigger the system and will contribute to the final sample (see discussion in section 4.C). The requirements imposed on the trigger will eliminate events with charged particles (π^+, p) associated to the K^o production or converted γ's from π^o's, that reach the anticoincidence counter behind the target.

A rough calculation permits to evaluate the contribution, in units of the "elastic" event rate:

from N^*	K^o production	$\sim$ 30%
from K^*	nucleon production	$\sim$ 10%
from non resonant π	production	$\sim$ 10%

K^+p cross section are taken from ref. 11. K^+n ones are assumed of the same order. Kinematical and geometrical cuts are applied as for "elastic" events. Nuclear π interactions have been taken into account.

As already pointed out the above conclusions are strongly dependent on the assumptions about charge-exchange cross section on heavy nuclei.

We conclude that it will be necessary a preliminary measurement of the $K^{\pm}$ nucleus charge exchange cross section for various types of nuclei.

We think this could be easily done using the spark chamber apparatus of the Cern group tuned on $K_1^o \longrightarrow \pi^+\pi^-$ decay.

A χ^2 analysis has been performed in order to find the minimum $\Delta Q/\Delta S$ violation that is detectable in our experiment with a reasonable statistics.

χ^2 is calculated by comparing the experimental time distribution of the reconstructed events with "theoretical" curves (efficiency and experimental errors folded in) corresponding to different values of the parameters Re X, Im X.

The uncertainty of these parameters, resulting from statistics of 8500 Monte Carlo generated events, is $\pm$ .02 for Re X and $\pm$ .04 for Im X.

As appears from fig. 1, this represents a substantial improvement compared with the preceding results. Actually, with an event rate of .06 events/pulse, it seems possible to collect a statistics of 15.000 ÷ 20.000 events, which is

twice the value we have considered in the χ^2 calculations in a period of ten days CPS.

REFERENCE

(1-5) see table I

(6) J.S. Bell, J. Steinberger - Proceedings of the Oxford Conference 1965 (pag. 214).

(7) C. Alff-Steinberger et al. Phys. Lett. 21, 595 (1966)

(8) K.A. Brueckner Phys. Rev. 98, 1445 (1955)

(9) I. Butterworth et al. Phys. Rev. Lett. 15, 734 (1965)

(10) D. Luers et al. Phys. Rev. 133, B 1276 (1964)

(11) M. Ferro Luzzi et al. N. Cim. 36, 1101 (1965)

(12) B.M.K. Nefkens et al. Phys. Lett. 19, 706 (1966)

(13) P. Franzini et al. Phys. Rev. 140, B 127 (1965)

(14) B. Jordan - CERN Report 65 - 14 (1965)

Appendix I

The beam Cerenkov counters.

The identification of the particles in the beam will be performed by means of two threshold gas Cerenkov counters. We have compared the performances of several gases, and eventually we have decided to fill counters with ethylene. In order to specify the mechanical characteristics of the counters, we have calculated the mean number N_e of photoelectrons emitted by the photocatode of a 56 UVP tube coupled with a fused quartz window to the body of the Cerenkov detector (Fig. A1)

$$N_e \simeq 2\pi\cdot\alpha\, L \int_{\lambda_1}^{\lambda_2} \left(1 - \frac{1}{n^2\beta^2}\right) \frac{1}{\lambda^2}\, R(\lambda)\, T(\lambda)\, S_{11}(\lambda)\, d\lambda$$

where

α = fine structure constant

L = useful length of the counter (cm)

n = refractive index of the gas

λ_1 = 2000 Å

λ_2 = 6000 Å

$R(\lambda)$ = fraction of the produced photons reaching the quartz window

$T(\lambda)$ = transmission of the SiO_2 window

$S_{11}(\lambda)$ = photocatode quantum efficiency of the 56 UVP tube (see photomultiplier tubes - Philips Oct. 65)

$R(\lambda)$ has been assumed independent of λ and equal to 0.5: this value has been estimated to be conservative. In fact, for example, the reflectivity of evaporated A is very near to 90%.

$T(\lambda)$, on the other hand, has been carefully ($\pm$ 0.5%) measured and the results, just referring to the window we will use, are quoted in Table 1.

TABLE 1

λ	τ%	λ	τ%
225 nm	86.5	550 nm	93.2
250 nm	88.5	600 nm	93.1
275 nm	89.6	650 nm	92.8
300 nm	90.2	700 nm	93.0
325 nm	91.0	750 nm	93.4
350 nm	91.2	800 nm	94.0
275 nm	91.6	850 nm	94.0
400 nm	92.0	900 nm	94.3
450 nm	92.6	950 nm	94.3
500 nm	93.0	1000 nm	94.6

The light absorption in the gas itself has been disregarded. Neglecting dispersion, and using the above data, we obtain

$$N_e \simeq 70 \quad L \left(1 - \frac{1}{n^2 \beta^2}\right)$$

n is given by the Lorentz-Lorentz formula which (for $n \simeq 1$) reads

$$n = 1 + \frac{3}{2} \frac{R}{M} = 1 + 0{,}564 \rho \quad (\text{for } C_2 H_4)$$

where

R = molecular refraction

M = molecular weight

ρ = density of the gas

ρ as a function of the pressure is tabulated in "Thermodynamic function of gases" ed. by F.Din, London 1961. A temperature of 25°C has been assumed. The results of these calculation are summarized in Figs. A2, 3, 4.

Fig. A2 gives, as a function of β, the threshold pressure of $C_2 H_4$.

From Fig. A3 and A4 useful pairs of values of pressure

(p) and length (L) are deducible, with N_e as a parameter. Fig. A3 refers to pions, and Fig.A4 to Kaons.

In conclusion, the first Cerenkov, intended to detect only pions, will have a useful length L = 40 cm, a internal diameter of 15 cm and a $C_2 H_4$ pressure of about 9 atms.

The second counter, which has to detect both pions and Kaons, will be 40 cm long and filled with about 35 atms of ethylene. The mechanical details are visible in Fig. A1.

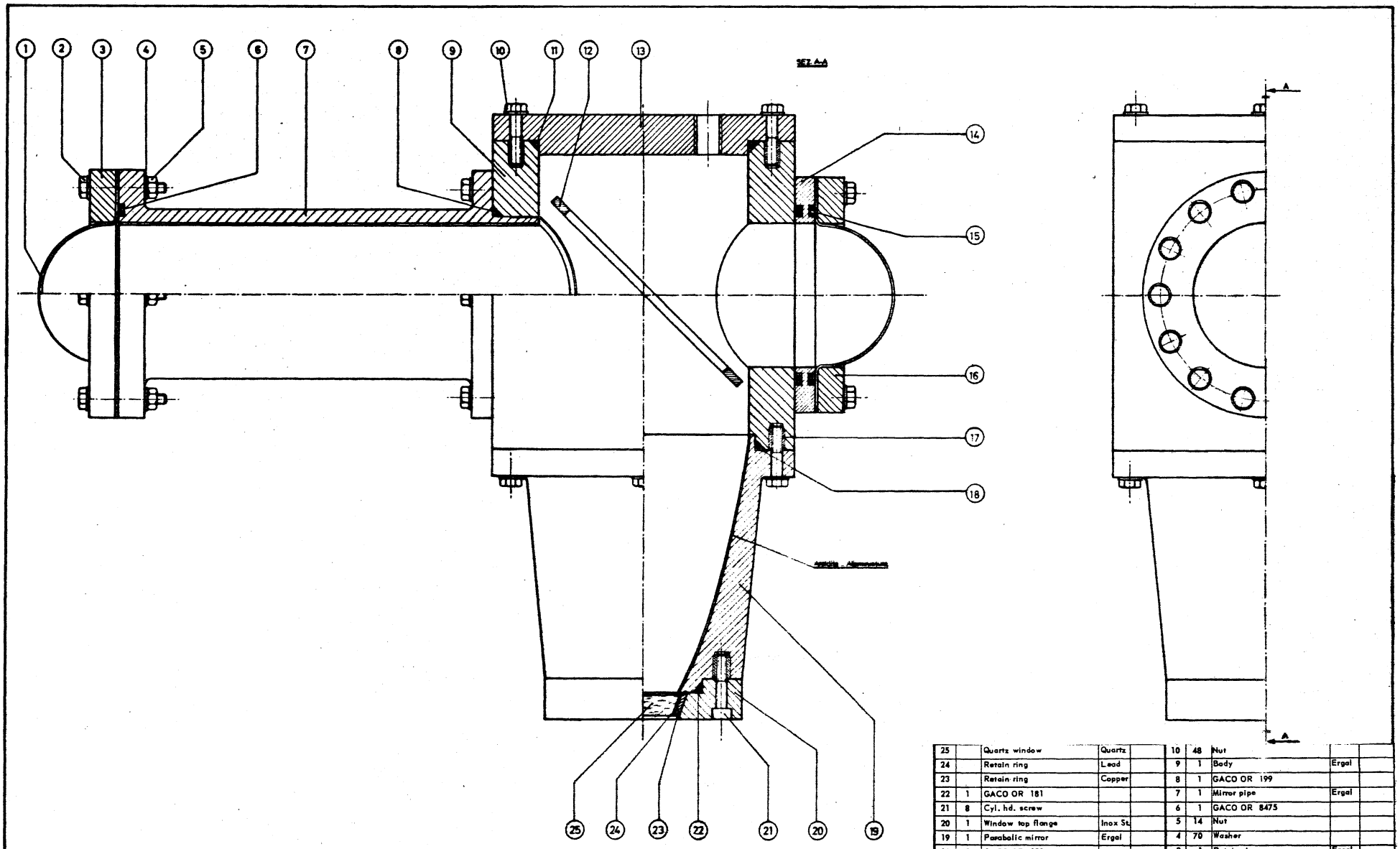

Item	Quan.	Descriptions	Mat.	Observ.
25		Quartz window	Quartz	
24		Retain ring	Lead	
23		Retain ring	Copper	
22	1	GACO OR 181		
21	8	Cyl. hd. screw		
20	1	Window top flange	Inox St.	
19	1	Parabolic mirror	Ergal	
18	1	GACO OR 229		
17	68	Threaded bush	Steel	
16	1	Retaing ring	Ergal	
15	2	GACO OR 8475		
14	1	Intermediate ring	Ergal	
13	1	Top flange	Ergal	
12	1	Mirror frame	Ergal	
11	1	GACO OR 225		
10	48	Nut		
9	1	Body	Ergal	
8	1	GACO OR 199		
7	1	Mirror pipe	Ergal	
6	1	GACO OR 8475		
5	14	Nut		
4	70	Washer		
3	1	Retain ring	Ergal	
2	28	Hex. hd. screw		
1	2	Spheric cover	Inox St	

CERENKOV COUNTER (CERN Mod.)

Scale 1:1

INFN - Torino - Servizi di Base

Modification

Signatures

Fig. 1 A

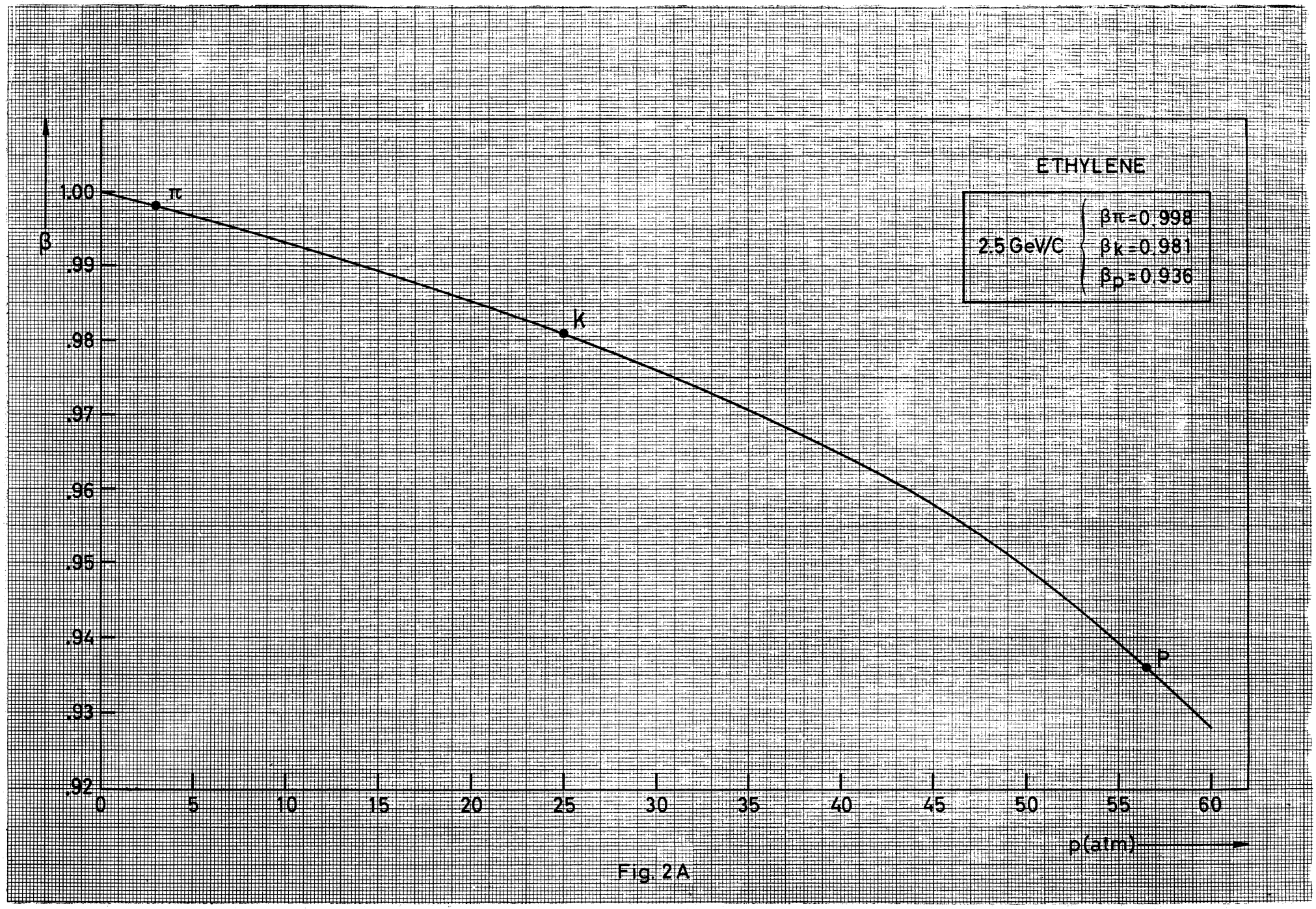
ETHYLENE
2.5 GeV/C
βπ = 0.998
βk = 0.981
βp = 0.936
β
1.00
.99
.98
.97
.96
.95
.94
.93
.92
π
K
P
0
5
10
15
20
25
30
35
40
45
50
55
60
p(atm)

Fig. 2A

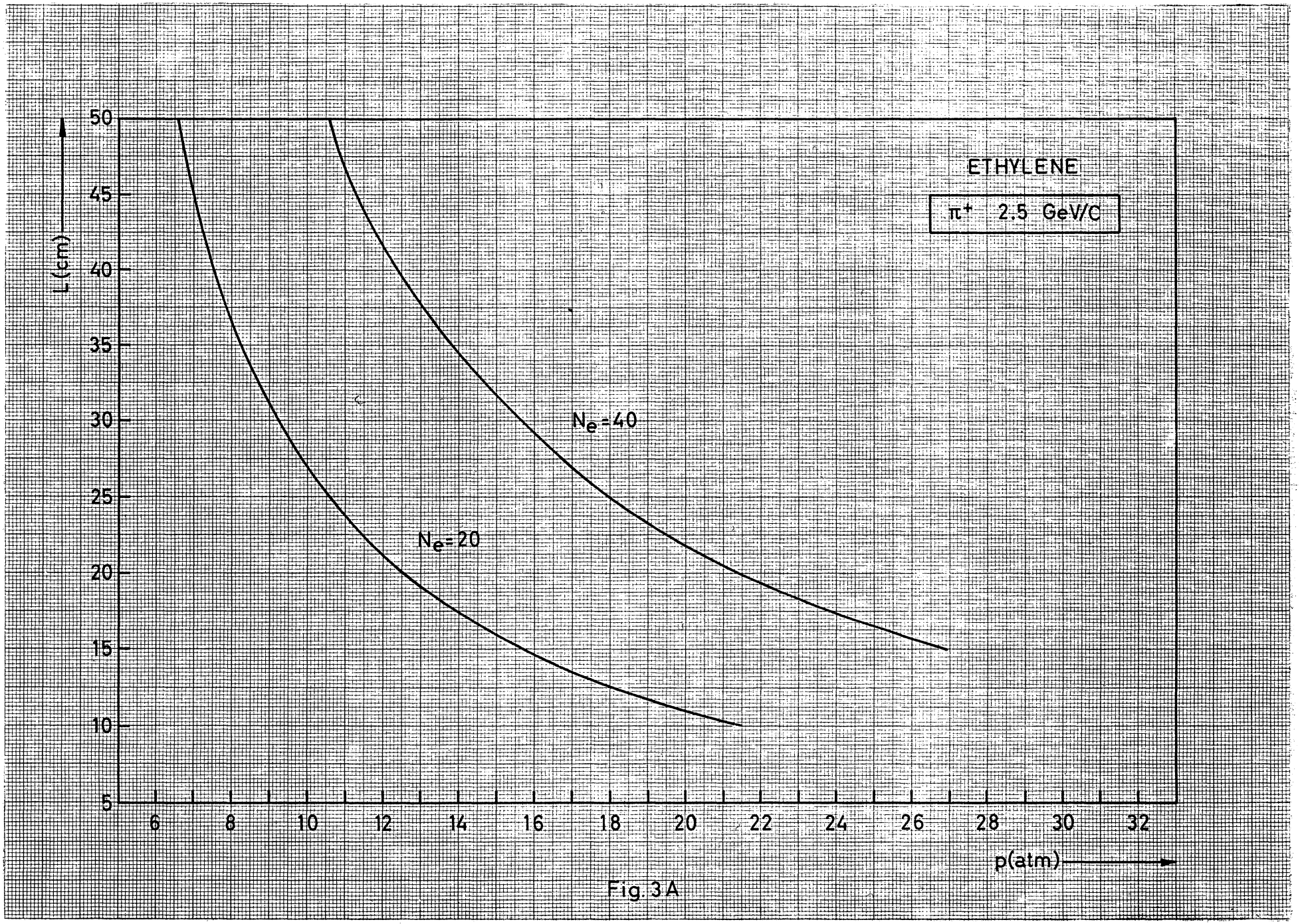
ETHYLENE
π+ 2.5 GeV/C
L (cm)
50
45
40
35
30
25
20
15
10
5
6
8
10
12
14
16
18
20
22
24
26
28
30
32
p(atm)
Ne=40
Ne=20

Fig. 3A

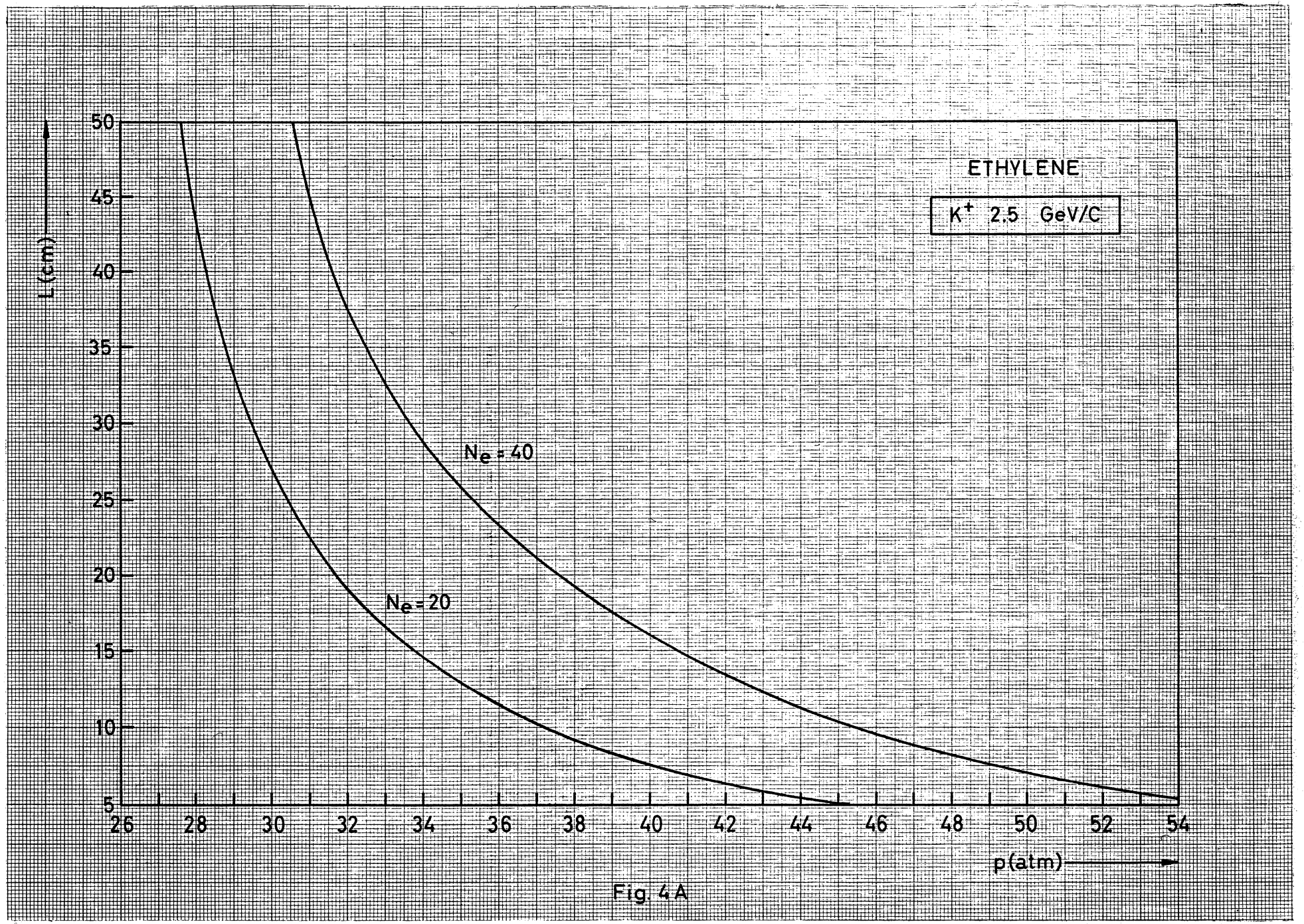
ETHYLENE
K+ 2.5 GeV/C
L (cm)
50
45
40
35
30
25
20
15
10
5
Ne = 40
Ne = 20
26
28
30
32
34
36
38
40
42
44
46
48
50
52
54
p(atm)

Fig. 4A

Appendix II

Lacking direct experimental information, we have calculated the yield of K^o's from a K^+ beam on copper using the following geometrical model.

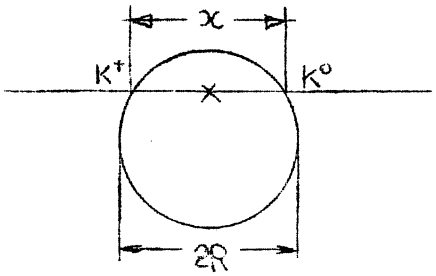

Let R be the nuclear radius of copper ($R = 1.1 \times 10^{-13} A^{1/3} = 4.4 \times 10^{-13}$ cm) and $\rho = \frac{3}{4\pi r_o^3} = 1.8 \times 10^{38}$ cm^{-3}. Let also λ_c be the mean free path of K^+ in nuclear matter for charge exchange scattering

$$K^+ + (n) \longrightarrow K^o + (P) \ ;$$

$\lambda^{(+)}$ the mean free path for a K^+ to scatter outside the angular interval accepted in the experiment; and $\lambda^{(o)}$ the same quantity for K^o's. We assume $\lambda^{(+)} = \lambda^{(o)} = \lambda$

A completely degenerate Fermi gas model has been assumed for the copper nucleus, with $P_F = 250$ MeV/c.

The effect of the Pauli principle has been calculated by taking all events which would be accepted by our apparatus and eliminating those for which the recoiling proton could still be inside the Fermi momentum sphere.

Thus, using the differential cross section for $K^+ \rightarrow K^o$ charge exchange, mentioned in the text, we have deduced that the Pauli principle reduces the total yield of events by a factor

$$f_p = 0,72$$

The mean free path λ has been obtained from known cross sections $\sigma_n (K^+ n \longrightarrow K^+ n)$ and $\sigma_p (K^+ p \longrightarrow K^+ p)$ on free

nucleons taking a weighted average in proportion to the number of protons and neutrons in the nucleus (see G. Kallén, Elementary particle Physics, ch. X). The effect of the Pauli principle can be neglected in this case as only high momentum transfers contribute to λ. In any case, the neglect of the Pauli principle will make the calculated λ shorter than its real value and thus produce an estimate which, if anything, is pessimistic in view of the scope of the experiment.

To a first approximation, largely justified by the smallness of the cross section for charge exchange, the probability for a K^+, entering the nucleus, to emerge as a K^o is

$$P = \frac{f_p}{2\lambda_c R^2} \int_0^{2R} e^{-x/\lambda}\, x^2\, dx$$

$$= \frac{f_p \lambda^3}{\lambda_c R^2} \left[1 - \left(\frac{1}{2}\left(\frac{2R}{\lambda}\right)^2 + \frac{2R}{\lambda} + 1\right) e^{-2R/\lambda}\right]$$

If only charge exchange processes were taking place ($\lambda = \infty$) and no account was taken of the Pauli principle ($f_p = 1$)

$$P \rightarrow P_\infty = \frac{4}{3}\frac{R}{\lambda_c}$$

The quantity

$$f_n = \frac{P}{P_\infty} = \frac{3}{4}\frac{\lambda^3 f_p}{R^3}\left[1 - \left(\frac{1}{2}\left(\frac{2R}{\lambda}\right)^2 + \frac{2R}{\lambda} + 1\right) e^{-2R/\lambda}\right]$$

can be seen as the number of "equivalent free neutrons", i.e. to how many free neutrons a copper nucleus corresponds for the process which is considered.

Taking

$$\lambda_c = (\sigma_0 \rho_n)^{-1} = 74 \times 10^{-13}\ \text{cm} \quad (\text{at } 2.5\ \text{GeV}/c)$$

then $f_n = 11 \times f_p \cong 8$.